FLUID MOTIONS IN A PERISTALTIC PUMP

by

Thomas Walker Latham
S.B., California Institute of Technology
(1964)

Submitted in partial fulfillment
of the requirements for the
Degree of Master of
Science
at the
Massachusetts Institute of
Technology
June, 1966

Signature of Author .....
Department of Mechanical Engineering

Certified by .....
Thesis Supervisor

Accepted by .....
Chairman, Departmental Committee
on Graduate Students

FLUID MOTIONS IN A PERISTALTIC PUMP

by

Thomas Walker Latham

Submitted to the Department of Mechanical Engineering on May 26, 1966, in partial fulfillment of the requirement for the degree of Master of Science

A peristaltic pump is a biological pump which employs periodic wavelike squeezing motions which travel along a vessel and force the contents of the vessel forward. The purpose of this investigation was to study three aspects of peristaltic pumping:

1) The input-output "gross" characterisitcs of the pump;

2) The fluid motions within the pump;

3) Fluid mixing within the pump due to circular or secondary flows.

The investigation proceeded along two lines: A theoretical analysis was made of a simplified model of peristaltic pumping; Peristaltic pumping was simulated with an experimental apparatus, and the data was compared to the theory.

The results of the experiment can be summarized as follows:

1) The pressure rise versus flow rate characteristics of the experimental pump correlated well with the theoretical analysis on a quantitative basis;

2) The fluid motions within the pump correlated with the theoretical analysis on a qualitative basis;

3) The investigation did not proceed far enough to produce more than speculative conclusions about fluid mixing within the pump.

TABLE OF CONTENTS

SYMBOLS

a average half-width, sinusoidal waveshape

b half-amplitude, sinusoidal waveshape

c speed of peristaltic wave

d half-width of peristaltic wave

λ wavelength

μ viscosity

p pressure

q volume flow rate in waveshape coordinate system

ρ density

t time

u x velocity in waveshape system

v y velocity in waveshape system

x,y cartesian coordinates, waveshape system

T.R. transport ratio

P.R. pressure ratio

$\hat{}$ signifies laboratory coordinate system

1. INTRODUCTION

1.1 Definition of Peristaltic Motion

In this age of specialization, it is often convenient to "let the expert do it". Submitting to expediency, this thesis begins with Webster's definition of peristaltic motion: "the peculiar worm-like wave motion of the intestines and other hollow muscular structures, produced by the successive contraction of the muscular fibers of their walls, forcing their contents onward".[1] The human ureter, a tube which connects the kidney to the bladder, is one of those "other hollow muscular structures" which pumps fluids by means of peristaltic motion. In this case the fluid is urine. The typical rate at which the human ureter pumps varies from almost nothing to about 4 ml. per minute, depending upon the urgency of the situation. The speed with which the peristaltic wave travels down the ureter is typically 3 centimeters per second. The frequency of the peristaltic waves can vary from ten per minute to less than one per minute. Further details about peristaltic motion of the human ureter will be contained in the next section of this paper.

1.2 Motivation of the Investigation

The interest in ureteral peristaltic motion stems from an observation which was made by Dr. Kass of Boston City Hospital. Dr. Kass noted that infections can travel from the bladder to the kidney, against the prevailing pumping action of the ureter, in a surprisingly short time. Experiments on rats showed that the infection could travel the length of the ureter (about 1.5 cm.) in about 5 hours.[2] The first question to ask is: Could ordinary diffusion be responsible for this effect? It would seem unlikely, since the infection must diffuse upstream faster than it is washed downstream by the flow of urine. However, perhaps the infection can diffuse up the boundary layer at the ureter wall. In order to investigate this possibility, let us determine if the infection could diffuse from the bladder to the kidney in 5 hours when the ureter is not pumping, i.e. when there is no adverse urine flow. The diffusion of the infection up the boundary layer would certainly be less rapid than diffusion under these conditions. An order-of-magnitude calculation is carried out in Appendix 1. It employs the elementary transient diffusion equation, $\frac{c}{c_i} = \text{erf}\,\frac{x}{2\sqrt{Dt}}$

and an order-of-mgnitude diffusivity constant which is typical for the diffusion of common inorganic materials in water. This calculation indicates that the concentration of infection at the kidney after five hours will be 0.5% of the concentration at the bladder. One might argue that since the infection reproduces, its diffusion rate would be increased by a source term. On the other hand, bacterial and viral particles are relatively large compared to inorganic molecules and will probably have a slower diffusivity constant than the molecules. On the whole, we conclude that diffusion up the boundary layer is not a convincing explanation of Dr. Kass's observations. The assumption of this investigation became that some other mechanism of fluid mixing exists within a peristaltic pump.

1.3 Purposes of the Investigation

The basic purpose of this investigation was to seek plausible mechanisms of augmented fluid mixing within a peristltic pump. In order to lay the foundations for this effort, the sub-objectives became:

a) investigate "gross" pumping characteristics;

b) investigate fluid motions within the pump;

c) investigate secondary fluid motions as a possible fluid mixing mechanism;

1.4 Methods of Investigation

The investigation was launched on both a theoretical and an experimental level. The theoretical attack was based on a simplified model of peristaltic motion and on the assumption that viscous forces overshadow the inertial forces in a peristaltic pump. The experimantal effort involved the construction of an apparatus to simulate peristaltic pumping. The theoretical and experimental approaches were combined in a comparison of the results.

1.5 Content of Following Sections

Section 2 will discuss theoretical models of peristaltic pumping, and their relevancy to the "real thing". Section 3 will discuss the basic theoretical approach, outlining the assumptions which were made and the results which followed. Section 4 will describe the experimental apparatus and the experimental procedure. Section5 will analyse the results of the theoretical and experimental investigations. It will discuss the gross characteristics of a peristaltic pump, the fluid motions within the pump, and the fluid mixing within the pump.

2. CHOOSING A MODEL

2.1 Introduction

Perhaps the most critical decision in this type of investigation is the selection of a model, for the model strongly influences the subsequent analysis. In model choosing, relevancy, which usually implies complexity, must be compromised with feasibility. This is the case in both theoretical and experimental work. The ideal is the model which is most relevant and yet still feasible.

2.2 Specific Information about the Human Ureter[3]

When one wants to develop a relevant model, the first thing to do is to ask some questions about the real world. The following information about the human ureter is divided into two categories; the structure of the ureter, and the characterisitics of ureteral peristaltic motion.

a) Structure:

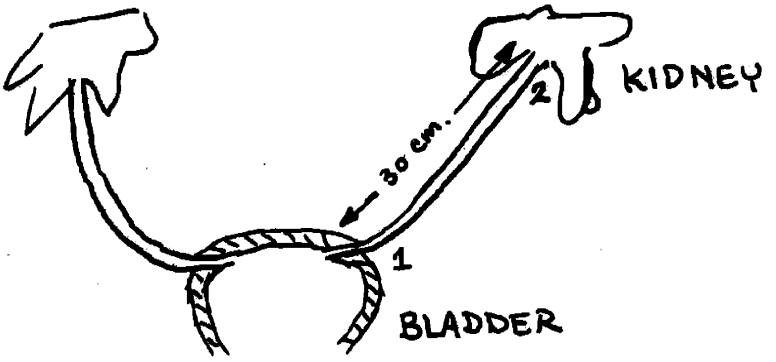

Figure 1

The significant dimensions of the ureter are:

length: 30 cm.

external diameter: 0.3 cm.

internal diameter: 0.05 cm.

A valve is situated at location 1, at the bladder end of the ureter (see figure 1). The valve consists of muscles in the wall of the bladder which can close the ureteral opening. A second valve seems to be situated at location 2, the kidney end of the ureter. It consists of a ring of muscles which close the ureter upon contraction. The wall of the ureter is composed of radial muscles and longitudinal muscles. The radial muscles form rings which circle the ureter. The longitudinal muscles lie along the length of the ureter.

b) Characteristics of ureteral peristaltic motion:

Wavespeed: varies from 1 to 6 centimeters per second

Diameter Reynolds Number: about 10 $\left(\frac{\rho c d}{\mu}\right)$

Frequency: varies from 10 to less than one wave per minute

Flow Rate: varies from negligible to 4 ml. per minute.

Waveshape: The waveshape depends partially upon the flow rate and the pressure level of the system. Under some circumstances, the wave may constrict the ureter completely. Under other dircumstances, it may not. The bulge part of the wave may vary from 1 centimeter in length for low flow conditions to 10 or 15 centimeters for high flow conditions. Usually only one wave is pre-

sent on the ureter at any time, although occasionally two waves are present for higher frequencies. X-ray photographs indicate typical waveshapes shown in figure 2.

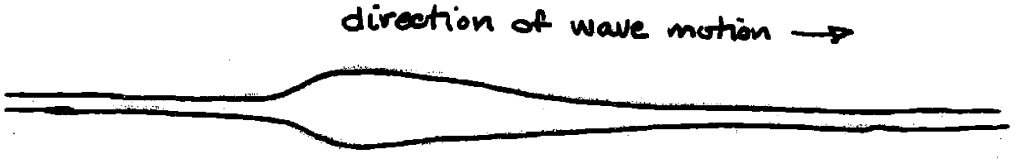

Figure 2

Longitudinal and Radial Motions: Both the radial and the longitudinal muscles are active during a peristaltic contraction. Saul Boyarsky reports, "Observation of the ureter at surgery or in movies conveys a definite impression: not only does the ureter contract during peristalsis, but it also glides to and fro lenthwise".[4]

2.3 Possible Models

We will begin the discussion of possible models by stating those things which were considered not feasible.

a) Valves were eliminated from the model. The characteristics of the biological valves were not known. Inclusion of valves did not seem desirable in this exploratory investigation.

b) Longitudinal motions of the wall were ruled out. First, longitudinal wall movements would have complicated the theory. Second, there was no easy way of simulating longitudinal motions experimentally.

c) Axially symmetric models were ruled out. There was no simple way of experimentally simulating an axially symmetric squeeze.

The most feasible model seemed to be the plane two dimensional model. A plane two dimensional tube is one which has characteristic length and width, but infinite height. In this way none of the properties of the system will depend upon the third cartesian coordinate, height. This model seemed feasible on an experimental level. Furthermore, the cartesian form of the equations for fluid motion are perhaps the easiest to work with.

Since the shape of peristaltic waves has not been determined very accurately, and since it changes depending upon the flow conditions, no common simplified waveshape seemed outstandingly more relevant than any other. Two simplified waveshapes were arbitrarily picked; the step wave and the sinusoidal wave. These two waveshapes are shown in figure 3.

STEP WAVESHAPE

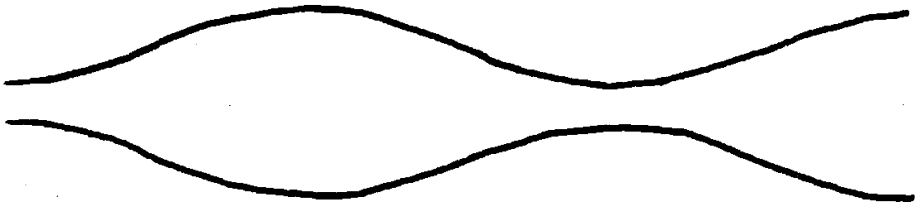

SINUSOIDAL WAVESHAPE

figure 3

In conclusion, the analysis will use a plane two dimensional model with both a step and a sinusoidal waveshape. The model has no valves and no wall motion in the longitudinal direction.

3. THEORY

3.1 Introduction

This section will contain two short demonstrations that peristaltic pumping depends upon a viscous mechanism and a somewhat longer discussion of a theoretical approach to peristaltic pumping.

3.2 Peristaltic Pumping and Viscosity

The purpose of the following two demonstrations is to show that a peristaltic pump is a viscous pump, in the sense that is will not work if $\mu = 0$.

a) First, let us consider a piece of tube which closes upon itself to form a circle as shown in figure 4.

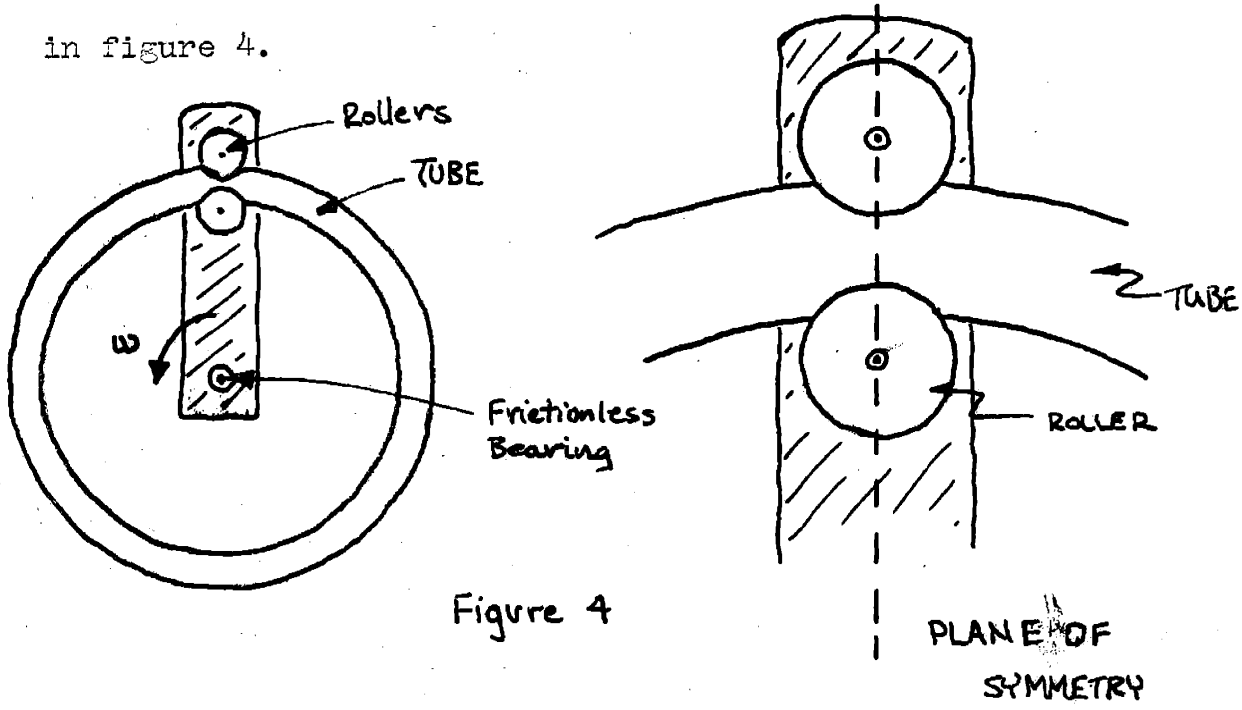

Figure 4

A radial bar extends from the center of the circle and has two frictionless rollers attached to it. The two rollers constrict the tube, thereby producing a squeeze. The bar is free to rotate on a frictionless bearing at the center of the circle, so that the rollers move along the tube. The tube is filled with an incompressible fluid. Let us assume that the rod is rotating with constant angular speed, w, in the counterclockwise direction. Let us assume that the fluid is inviscid. Then we ask the question; Will the peristaltic squeeze pump the fluid? The following line of argument shows that it will not. If we change coordinate systems by standing on the bar and rotating with it, then the wave will appear to be fixed with respect to the new coordinate system. In fact, the system will become a steady system; no property of the system will change with respect to time. If we further assume that gravitational forces are of no consequence, then the flow inside the tube becomes a simple Bernoulli flow in which the pressure is directly related to the scalar speed of the fluid. In a steady system the scalar speed is directly related to the crossectional area. Since the tube crossectional

area is symmetrical about the plane which contains the bar and is perpendicular to the paper, then the scalar speed must be symmetrical also. But if the scalar speed is symmetrical, then the pressure must be symmetrical. If the pressure is symmetrical with respect to this plane, then there can be no resultant force on the rollers perpendicular to the plane, and hence perpendicular to the bar. Now let us jump back to the original laboratory coordinate system. If there is no resultant force acting perpendicular to the bar, then no work is required in order to keep the bar rotating. But if the bar keeps rotating without anyone cranking it, then certainly the bar is not doing any work on the fluid. If the bar is not doing any work on the fluid, then it is not pumping the fluid.

We notice that if the fluid had been viscid, then the pressure distribution would not have been symmetrical and a force would have existed perpendicular to the bar. In this case the bar would have been transmitting energy to the fluid. Pumping would have occurred.

b) The second demonstration will give the reader a physical feel for how a peristaltic pump works. Consider a tube connecting two reservoirs as shown in figure 5. A squeeze in the tube is moving towards the right with speed c.

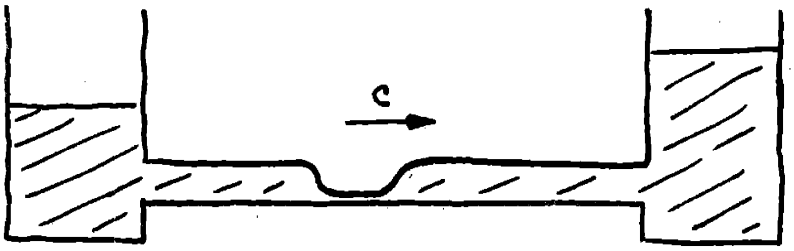

Figure 5

If the squeeze completely closes the tube, then it is obvious that all of the fluid in the tube will be pushed into the reservoir at the right. On the other hand, if the squeeze does not quite close the tube completely, but leaves a narrow passage, then most of the fluid will be pushed into the reservoir at the right but a small amount will seep back through the passage. Only a small amount will seep back since large viscous forces will occur in the narrow passage. This demonstrates a fundamental characteristic of peristaltic pumping. A small amount of fluid moving backwards

under the pinch provides enough force to push a larger amount of fluid forward through the bulge.

3.3 Theoretical Analysis of the Sinusoidal Plane Two Dimensional Model

As mentioned above, both the sinusoidal and step waveshape models were considered during the course of this investigation. However, experimental data was taken only for the sinusoidal model. Therefore this section will outline the theoretical approach only for the sinusoidal model. It will specify the assumptions involved and present the results. The details of the theoretical analysis for both the sinusoidal and the step waveshape models are given in Appendix 2.

A) WAVESHAPE COORDINATE SYSTEM

Figure 6 shows the sinusoidal waveshape plane two dimensional model. The analysis begins in a coordinate system fixed to the wave, the waveshape coordinate system,

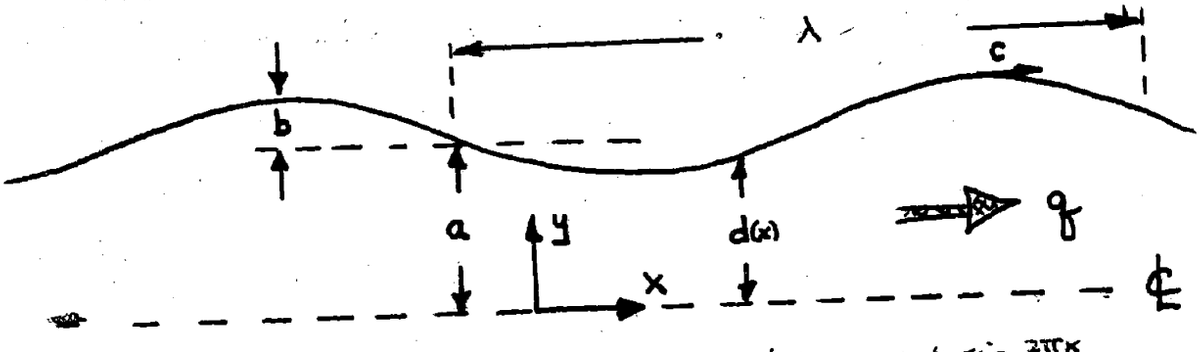

Figure 6

$$d(x) = a + b \sin \frac{2\pi x}{\lambda}$$

in which the system is steady. Note that in this coordinate system the tube wall moves to the right with speed c. This system is truly steady only if the wall has no ends.

The theoretical analysis begins with the most general form of the Navier Stokes equation for fluid motion. We whittle it down to a mere shadow of its former self with 7 assumtions. The assumptions are:

1) Gravitational forces are of no consequence;
2) The density is constant over space and time;
3) The viscosity is constant over space and time;
4) There is no z dependency and no z velocity;
5) There is no time dependency (the tube is infinitely long);
6) The wavelength is long compared to the width ($a \ll \lambda$);
7) The diameter Reynolds number is small ($\frac{\rho u a}{\mu} \ll 1$);

The first five assumptions reduce the Navier Stokes equation to a familiar steady state, two dimensional cartesian form with inertial terms, viscous terms, and pressure gradient terms. Assumptions 6 and 7, combined with an order-of-magnitude analysis, reduce the equation still further to the form:

$$\frac{\partial p}{\partial x} = \mu \frac{\partial^2 u}{\partial y^2}$$ Equation 3.1

Thus, the implications of the above assumptions has been that fully developed parabolic Pouseuille flow exists everywhere in the tube.

Integration of equation 3.1 with the appropriate boundary conditions gives u as a function of x and y. The conditions of incompressibility and continuity can be used to determine v from u. They are:

$$u = c - \frac{1}{2\mu} \frac{dp}{dx} \left[d^2 - y^2 \right]$$ Eq 3.2

$$v = \frac{3}{2} \frac{d(d)}{dx} \left[\frac{q}{d} \frac{y}{d} + \left(\frac{2}{3} c - \frac{q}{d} \right) \frac{y^3}{d^3} \right]$$ Eq 3.3

From u and v the stream function is derived:

$$\psi = \frac{1}{2} c a \frac{y}{d} \left[\frac{d}{a} \left(1 - \frac{y^2}{d^2} \right) - \frac{q}{ac} \left(3 - \frac{y^2}{d^2} \right) \right]$$ Eq 3.4

B) Laboratory Coordinate System

We now change back to the laboratory coordinate system, as shown in figure 7.

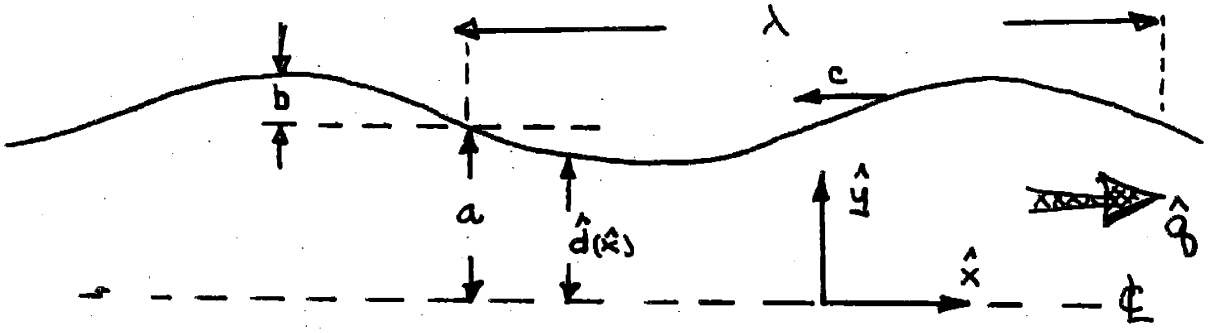

Figure 7

The fluid motions are not steady in the laboratory coordinate system. In this system the walls are stationary and the wave moves towards the left at speed c. The laboratory coordinate system is related to the waveshpae coordinate system by the equations:

$$\hat{x} = x - ct$$
$$\hat{y} = y \qquad \text{Eq 3.5}$$

Using these relationships we find that:

$$\hat{u}(\hat{x},\hat{y}) = u(\hat{x}+ct,\hat{y}) - c = \frac{3}{2}\left[\frac{q}{d} - c\right]\left[1 - \hat{y}^2/\hat{d}^2\right] \qquad \text{Eq 3.6}$$

$$\hat{v}(\hat{x},\hat{y}) = v(\hat{x}+ct,\hat{y}) = \frac{3}{2}\frac{d(\hat{d})}{d\hat{x}}\left[\frac{q}{d}\frac{\hat{y}}{\hat{d}} + \left(\frac{2}{3}c - \frac{q}{d}\right)\frac{\hat{y}^3}{\hat{d}^3}\right] \qquad \text{Eq 3.7}$$

$$\hat{\psi}(\hat{x},\hat{y}) = \frac{1}{2}ca\frac{\hat{y}}{\hat{d}}\left[\frac{\hat{d}}{a}\left(1 - \frac{\hat{y}^2}{\hat{d}^2}\right) - \frac{q}{ac}\left(3 - \frac{\hat{y}^2}{\hat{d}^2}\right)\right] \qquad \text{Eq 3.8}$$

where:

$$\hat{d} = d(\hat{x}+ct) = a + b\sin\frac{2\pi}{\lambda}(\hat{x}+ct) \qquad \text{Eq 3.9}$$

An interest in the gross characteristics of the pump compels us to develop a relationship between a dimensionless pressure rise and a dimensionless flow output. The dimensionless pressure rise, called the pressure ratio, is defined as the pressure rise over one wavelength divided by an arbitrarily chosen

reference pressure rise. This is chosen to be the maximum pressure rise which the pump can develop across one wavelength. Similarly, the dimensionless flow output, called the transport ratio, is defined as the net volume of fluid transported during one cycle divided by an arbitrarily chosen reference volume. The reference volume is that volume which lies beneath the bulge, as shown by the shaded area in figure 8.

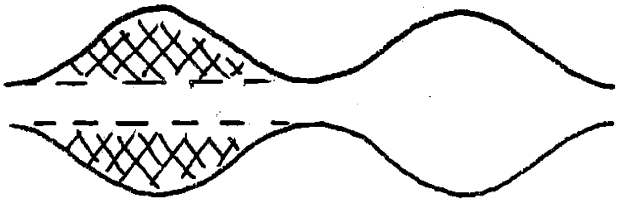

Figure 8

For normal pump operations the pressure ratio can vary between zero, when there is no pressure rise across the pump, to one, when the pump is producing its maximum pressure rise. The transport ratio will vary between zero, when there is no net flow emerging from the pump output, to some other value which is not immediately apparent, when the maximum amount of flow is occurring. The pressure ratio is found after integrating the pressure gradient with respect to x over one wavelength. The transport ratio is found after integrating the output flow rate with respect to t over one cycle. Combination yields

the following relationship between them:

$$T.R. = \frac{a}{b}\left[\frac{3}{2\frac{a^2}{b^2}+1}\right]\left[1 - P.R\right] \qquad \text{Eq 3.10}$$

In conclusion, the theoretical approach consisted of the following steps. A series of assumptions was used to simplify the Navier Stokes equation. The fluid velocities were derived in both the steady waveshape coordinate system and the unsteady laboratory coordinate system. Finally, a relationship between dimensionless pumping characteristics was derived.

4. EXPERIMENTAL WORK

4.1 Introduction

This section will discuss the experimental aspects of the investigation. It will outline the limitations and the objectives of the design of the experimental apparatus. Then it will briefly describe the experimental apparatus. Finally, it will outline how measurements were taken.

4.2 Apparatus Design Limitations and Objectives

a) There were four main limitations upon the design of the experimental apparatus. First, the peristatic tube had to be substantially two dimensional. In other words, the z dimension had to be quite large compared to the y dimension. Second, no longitudinal movement of the tube walls could be allowed. Third, there were to be no valves. Fourth, the tube had to have dimensions such that a low Reynolds number could be obtained.

b) There were six main design objectives. It was desirable to be able to vary: 1) the waveshape, 2) the wavelength, 3) the wave amplitude, 4) the wave speed. In addition, the peristatic tube was to be: 5) clear and 6) accessible.

4.3 Description of Experimental Apparatus

The following description of the appartus will be cursory. Appendix 3 contains more detailed information about the apparatus, including specific dimensions, operating ranges, fluids used, etc. We divide the appartus into its functional parts for the following description.

a) Producing the Peristaltic Wave: The part of the apparatus which produced the peristaltic wave is shown in Figure 9.

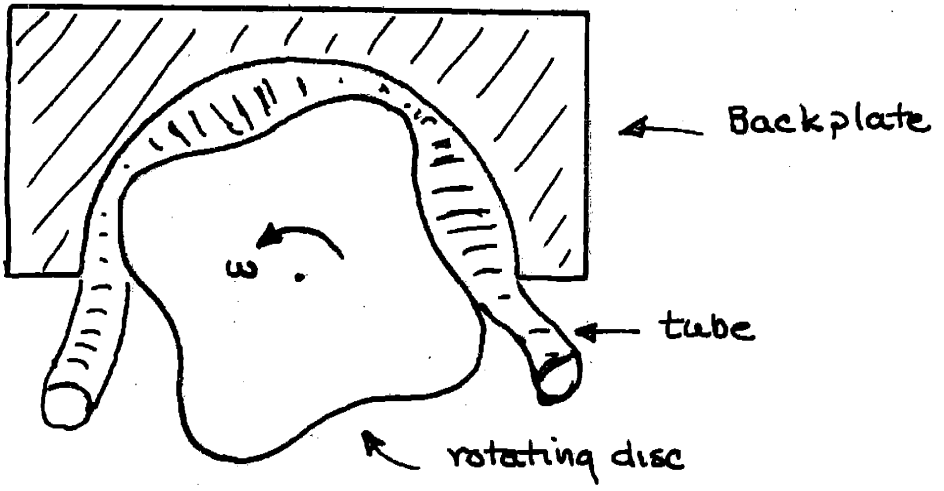

Figure 9

The rigid backplate served as a semi-circular template, to which the peristaltic tube was cemented. A rotating disc was positioned so that the peristaltic tube was constrained between it and the backplate. As shown in the figure, the rotating disc had lobes on it, so that it was analogous to a cam. When the disc was turned, the squeeze traveled along

the tube. The disc was constructed so that there was no direct sliding motion along the tube wall. The length, shape, and amplitude of the lobes were variable. In addition the speed of rotation of the disc was variable. In this way four of the design objectives were satified. Although in the Figure the curvature of the peristaltic tube seems to distort its waveshape, in the actual case the dimensions were such that the curvature was unimportant.

b) Measuring the Pressure Rise and Flow Rate: As shown in Figure 10, a reservoir was attached to each end of the peristaltic tube.

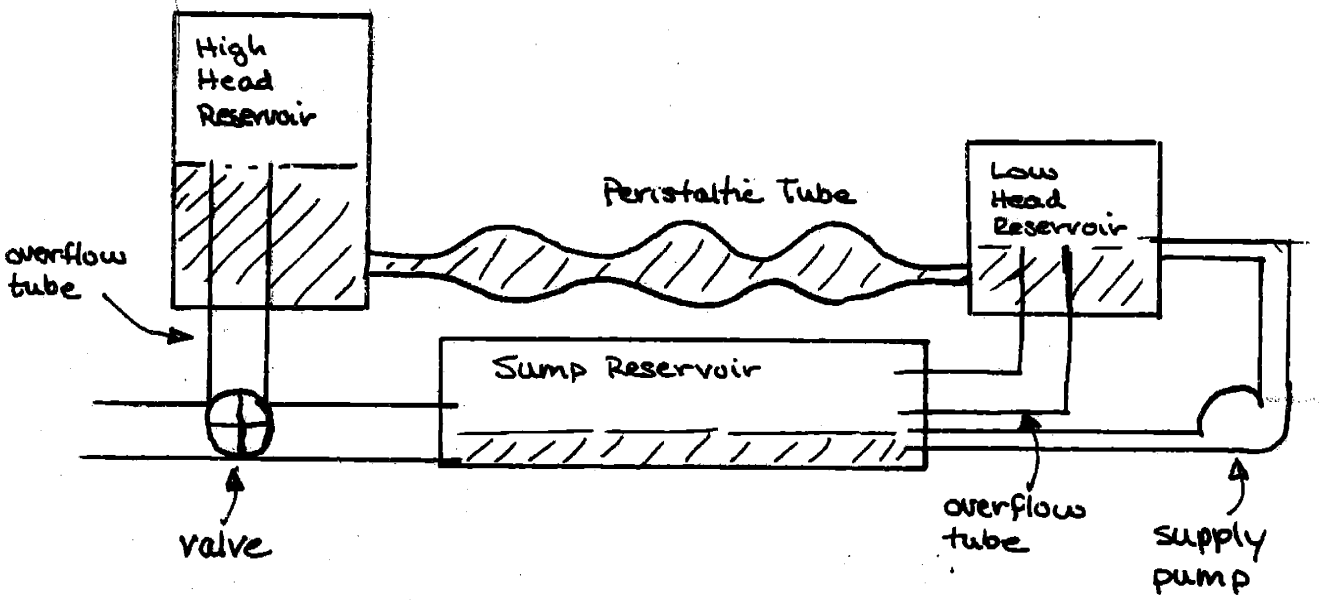

Figure 10

The height of the fluid in the "low head" reservoir was kept constant. This was accomplished by using

a centrifugal supply pump and an overflow drain. The level of the fluid would never go above the overflow drain, but the supply pump never allowed it to go beneath. The height of the fluid in the "high head" reservoir was measured. The difference in heights was a measurement of the pressure rise across the peristaltic pump. The height of the overflow drain in the "high head" reservoir could be varied so that the peristaltic pump could run with different pressure rise conditions. The overflow from the "high head" reservoir was the net flow of the peristaltic pump. The diagram shows a valve on the high head overflow drain. The net flow per cycle of the pump was measured by diverting the overflow through this valve and into a graduated cylinder.

c) Observing Fluid Motions Within the Peristaltic Pump: The peristaltic tube was made of clear polyvinylchloride. Hence, it was possible to observe the fluid motions inside the pump by introducing dye through the wall of the tube with an hypodermic needle.

4.4 Experimental Procedure

Six quantities had to be measured to define each data point.

1) The geometry of the wave (Waveshape, amplitude, wavelength);

2) Wavespeed;

3) The differential pressure head between the reservoirs;

4) The volume flow per cycle;

5) The viscosity;

6) The density;

First a fluid was poured into the system. This fixed the density and to a certain extent the viscosity (the viscosity was heavily dependent upon temperature). Then the geometry was set. Tests were made with four different geometries. Last, the wavespeed and pressure rise were varied, and the volume flow measured for each case. The procedure was set up in this sequence because the flow was the variable least easy to control.

5. ANALYSIS OF RESULTS

5.1 Introduction

This section will compare the theoretical and experimental results for the gross characteristics of the peristaltic pump, presenting the data on four graphs. Then it will discuss the theoretical and observed fluid motions within the pump. Last, it will speculate about the possibility of secondary flows within the pump.

5.2 Gross Characteristics of the Pump

a) Dimensional considerations:

We will begin the discussion of the gross pump characteristics by determining the relevant dimensionless parameters. As a first approximation, we employ the Pi Theorem approach to dimensional analysis. The physical variables are: $\Delta P, \rho, \mu, c, q, a, b, \lambda$. Primary dimensions are mass, length, and time. Hence, we take u, c, and a as independent and form dimensionless ratios with the other variables. We

find:

pressure ratio	$\frac{\Delta P}{\mu c / a}$	Reynolds No.	$\frac{\rho c a}{\mu}$
Flow ratio	$\frac{q}{a^2 c}$	geometrical ratios	$\frac{\lambda}{a}$, $\frac{b}{a}$

These are the five groups of relevant dimensionless parameters. The Pi Theorem states that any one can be expressed as a function of the other four. We note that the pressure ratio and the transport ratio defined in section 3.3 have the same dimensional form as the pressure ratio and the flow ratio here, and that the former are refinements which are more appropriate for our specific case. The analysis demonstrates that the Reynolds number is a significant parameter also. We decide to refine it in a similar manner. Taking the differential form:

$$\text{Reynolds number} = \frac{\rho u \, \partial u/\partial x}{\mu \, \partial^2 u/\partial y^2}$$

and using u from section 3.3, we obtain the result:

$$\text{Reynolds number} = \frac{\rho c (a-b)}{\mu} \frac{a-b}{a} \frac{a-b}{\lambda} \frac{3\left[\frac{2}{3} - \frac{b}{a} T.R.\right]\left[1 - \frac{b}{a} T.R.\right]}{\left[1 - T.R.\right]} \qquad \text{Eq 5.1}$$

The derivation of this Reynolds number is explained in Appendix 2. Due to assumptions made in the derivation, this expression is valid only for:

$$0 \leq T.R. \leq \frac{a}{b}\left[\frac{3}{2\frac{a^2}{b^2}+1}\right]$$

This expression shows that the Reynolds number depends

upon a characteristic diameter Reynolds number, two geometrical ratios, and a coeffecient in T.R. However, we note that in the operating range of the pump, the coefficient in T.R. changes only slowly with T.R.

We will use the refined parameter groups, for presenting the results.

b) Presentation of Data:

From the above discussion we have 4 relevant parameters groups which can be varied. In the presentation of data, we will portray the variation in each parameter group in the following way. Each graph represents a different geometry. Graph 1 has a medium pinch (bulge thichness to pinch thickness is 2:1) and 4 wavelengths between the ends. Graph 2 has a medium pinch and 1 wavelength between the ends. Graph 3 has a severe pinch (bulge thickness to pinch thickness is 5:1) and 4 wavelengths between the ends. Graph 4 has a severe pinch and one wavelength between the ends. On each graph the variation in Reynolds number is portrayed by different symbols. The pressure ratio is plotted on the ordinate and the transport ratio on the abscissa. The theoretical relationship between them, expressed in equation 3.10, is shown by the heavy black line on each graph.

GRAPH 1

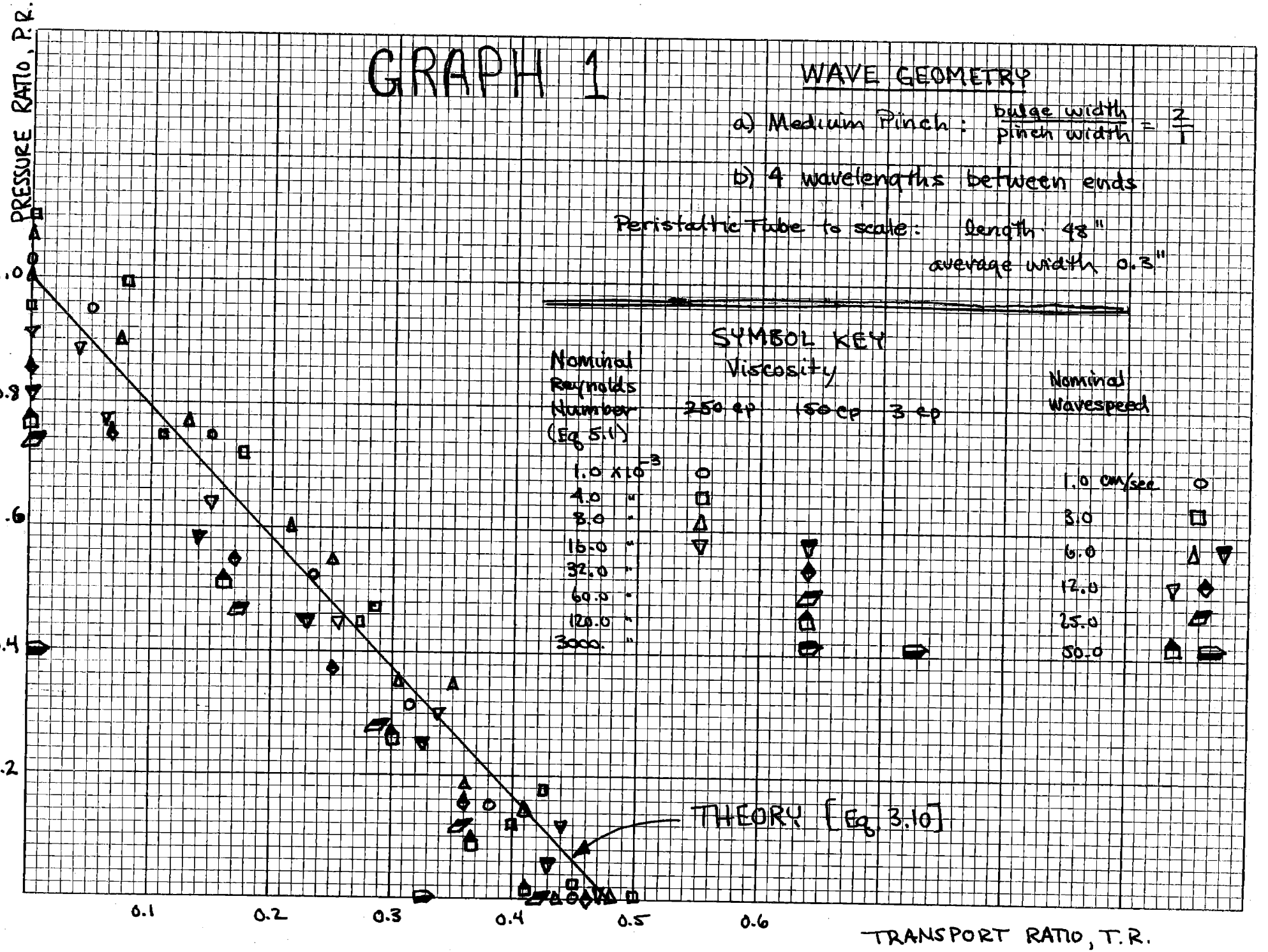

GRAPH 2

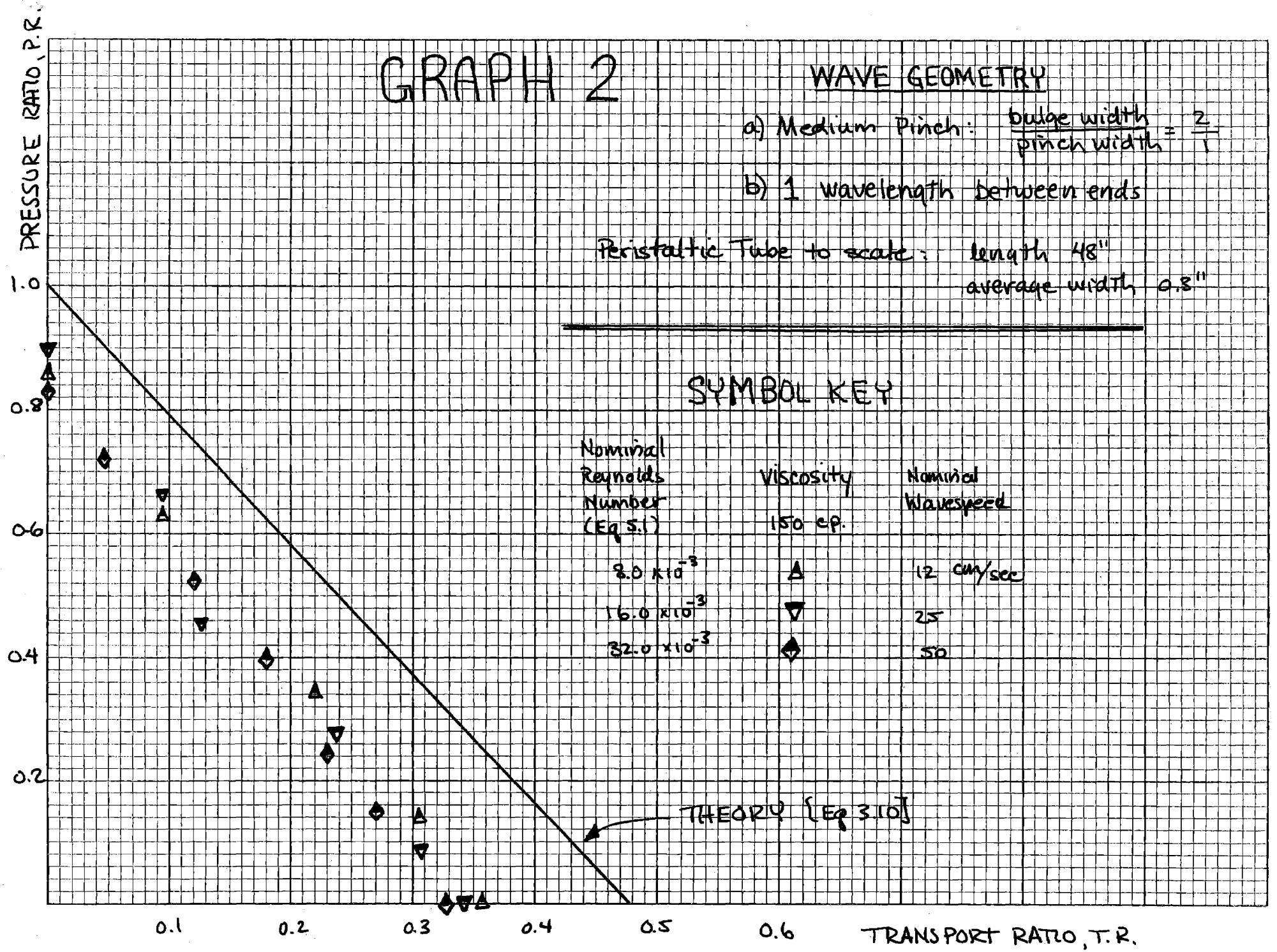

WAVE GEOMETRY

a) Medium Pinch: $\frac{\text{bulge width}}{\text{pinch width}} = \frac{2}{1}$

b) 1 wavelength between ends

Peristaltic Tube to scale: length 48"
average width 0.8"

SYMBOL KEY

Nominal Reynolds Number (Eq 5.1)	Viscosity 150 cp.	Nominal Wavespeed
8.0×10^{-3}	△	12 cm/sec
16.0×10^{-3}	▽	25
32.0×10^{-3}	◇	50

GRAPH 3

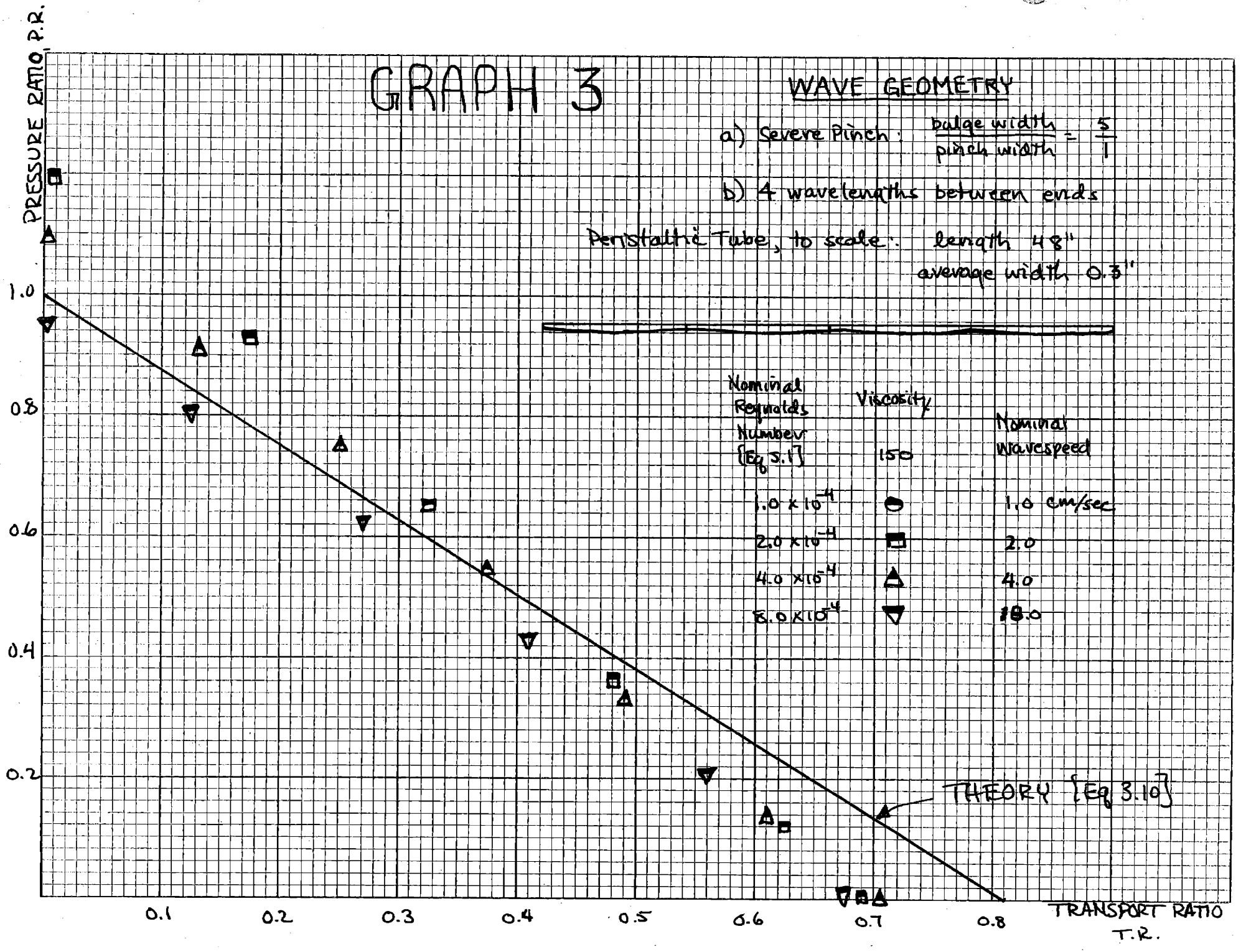

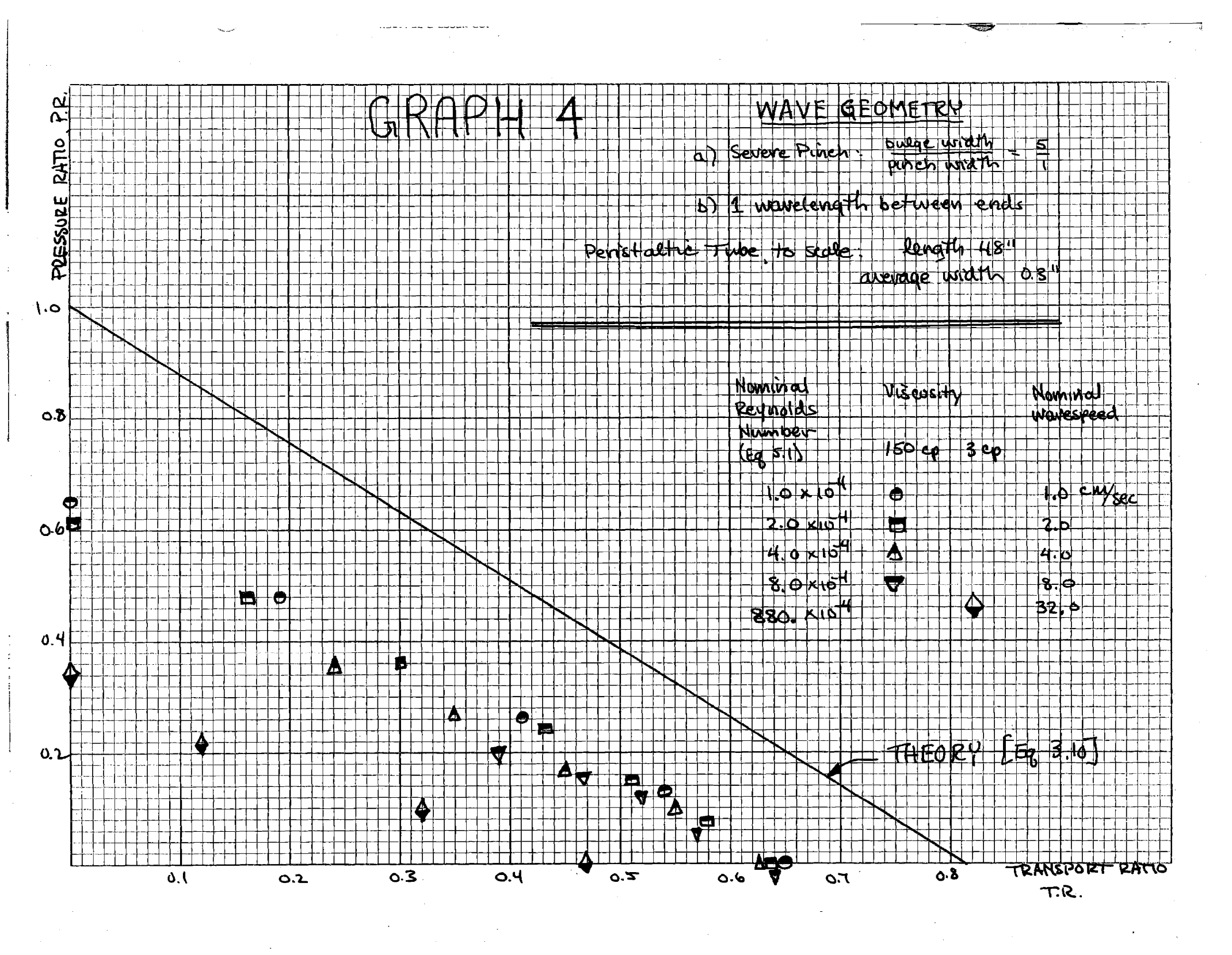
GRAPH 4
WAVE GEOMETRY
a) Severe Pinch: bulge width / pinch width = 5/1
b) 1 wavelength between ends
Peristaltic Tube, to scale: length 48"
average width 0.3"
Nominal Reynolds Number (Eq 5.1)
Viscosity
150 cp
3 cp
Nominal wavespeed
1.0 x 10^-4
2.0 x 10^-4
4.0 x 10^-4
8.0 x 10^-4
880. x 10^-4
1.0 cm/sec
2.0
4.0
8.0
32.0
THEORY [Eq 3.10]
PRESSURE RATIO P.R.
TRANSPORT RATIO T.R.
1.0
0.8
0.6
0.4
0.2
0.1
0.2
0.3
0.4
0.5
0.6
0.7
0.8

c) Analysis of the Graphs:

i) End Effects;

The theoretical results rest upon an assumption of steady state conditions in the wave-shape coordinate system. This implies that the tube is infinitely long, that it has no ends. An experimental test of the end effects was conducted. Graph 1 shows a medium pinch geometry which has 4 wavelengths between the ends. Graph 2 has only one wavelength between the ends. We would expect the effect of the ends to be more important in the second case. It is reasonable that the effect of the ends would be to lower the effectiveness of the pump since at the end the fluid squirts into the reservoir and dissipates some kinetic pressure head in a non-productive way (turbulence, etc.) Comparison of Graphs 1 and 2 shows that the increase in end effect lowered the maximum transport ratio by about 30% but did not affect the maximum pressure ratio much. Comparison of Graphs 3 and 4, which is the counterpart situation for the severe pinch case, shows the maximum transport ratio lowered by about 10% and the pressure ratio lowered by about 40%.

ii) Side Effects;

The theoretical analysis assumed there was no z depencency in the fluid motions. This implied that the peristaltic tube was infinitely deep in the z direction. Of course, the experimental tube had a top and a bottom. In the experiment the ratio of the depth to the average width was on the order of 8:1. Although this would be adequate from strictly viscous considerations, another effect appears. Since the tube has a constant perimeter, the depth must decrease as the width increases when a bulge advances. The effect of the decrease in depth at the bulge was to lower the transport ratio because the volume of the bulge was decreased. Furthermore, the stiffness of the tube caused the crossection to have a rounded top and bottom, as shown in figure 11.

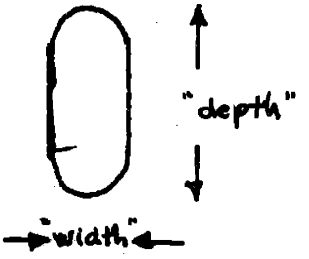

Figure 11

This affected the average dimensions of the pinch as well as the volume of the bulge. Both effects tended to lower the transport ratio.

In total, the side effects may be a partial explanation of the fact that the maximum theoretical

transport ratio was never achieved in the experimental test.

iii) Reynolds Number Effect;

The variation in Reynolds number is shown by different symbols on the graphs. The theoretical derivation assumed a very low Reynolds number, and then showed that the relationship between pressure ratio and transport ratio is independent of Reynolds number. Hence, we would expect in the experiments to find that for low enough Reynolds numbers, a change in Reynolds number would not change the data points. We would also expect to find a transition Reynolds number where the theory loses validity and where further increases in Reynolds number would adversely affect the effectiveness of the pump. The graphs seem to indicate that the lowest experimental Reynolds numbers were lower than the transition point, within the limitations of experimental accuracy. The highest Reynolds number tested shows a decisive drop in pump effectiveness, as anticipated. Both c and μ were varied in the experiment. Hence some data points represent different c's and μ's, but the same ratio of c/μ and hence the same Reynolds number. This was a method of checking that Reynolds number influence was independent of these variables.

iv) Other Effects;

First, the difficulty of obtaining

accurate values of viscosity in the face of temperature changes caused the experimental data to spread as it approached the maximum pressure rise end of the curves. Second, for some unexplained reason, the experimental data seemed consistenly to curve slightly downward as it approached that end. Last, a set of data taken on one day seemed to cohere better than data taken on different days. This can probably be explained by the temperature differences from day to day and the relaxation of the apparatus.

5.3 Fluid Motions Within The Pump

Theoretical expressions for the fluid velocities inside the pump are given in section 3.3. We can use these expressions in order to find the velocity profiles inside the pump at various positions and for various conditions. Let us use the expressions for the velocities in the laboratory coordinate system, which we remember is the unsteady coordinate system. At the risk of creating some initial confusion, we

change the expressions of 3.3 so that the wave is moving towards the right, and therefore has a positive velocity. We do this so that there will be no confusion about whether a positive fluid velocity is one which is moving in the direction of the wave or in the positive coordinate direction. Now they are both the same thing. The u velocity profile is shown in Figure 12 for wave geometry #1 and #3, each for T.R. = 0 and T.R. = $\frac{a}{b}\left[\frac{3}{2\frac{a^2}{b^2}+1}\right]$ = T.R.$_{max.}$ From these diagrams we notice that negative velocities occur at the pinch. Also, the negative velocity is greater for the T.R. = 0 cases. These profiles are the "instantaneous" profiles. The profile is fixed to the waveshape, and moves with it to the right.

These observations help to explain how viscosity causes the peristaltic pump to work. Back flow in the pinch gives enough pressure rise from viscous effects to compensate for the pressure drop due to forward motion in the bulge. At the pump outlet, as the pinch passes, the fluid is flowing backward into the pump. But as the bulge passes, a large volume of fluid is expelled, more than compensating for the previous back flow, and giving rise to a net flow

FLUID VELOCITY PROFILES

GEOMETRY 1: $\frac{\text{bulge width}}{\text{pinch width}} = \frac{3}{1}$

Fluid velocity profiles are scaled to the standard wavespeed velocity, c.

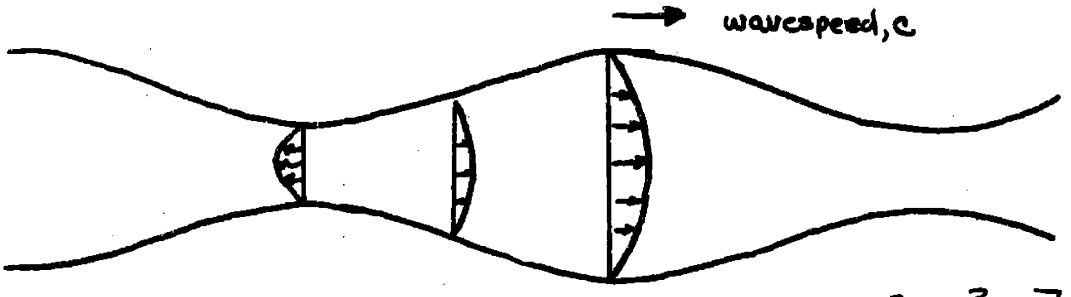

$$T.R. = T.R._{max} = \frac{a}{b}\left[\frac{3}{2\frac{a^2}{b^2}+1}\right] = .48$$

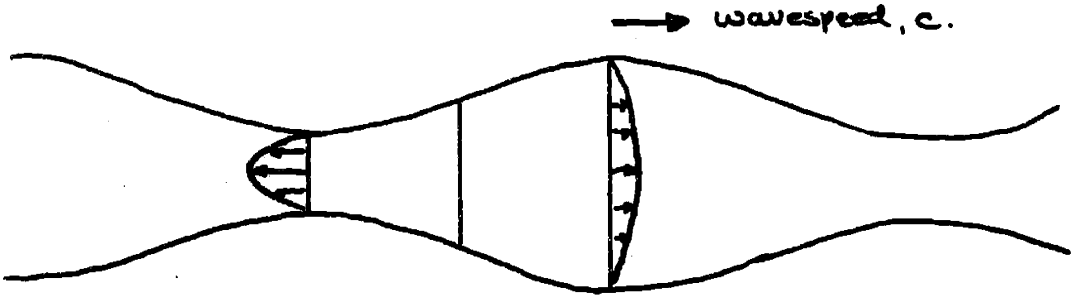

$$T.R. = 0$$

Figure 12

FLUID VELOCITY PROFILES

GEOMETRY 3 $\frac{\text{bulge width}}{\text{pinch width}} = \frac{5}{1}$

Fluid velocity profiles are scaled to the standard wavespeed velocity, c.

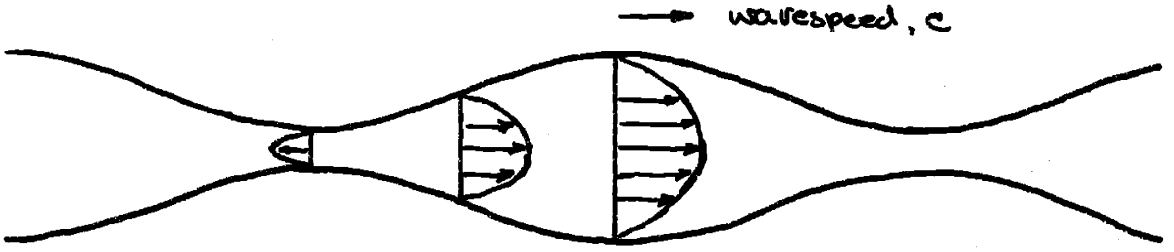

$$T.R. = T.R._{max} = \frac{a}{b}\left\{\frac{3}{2\frac{a^2}{b^2}+1}\right\} = .81$$

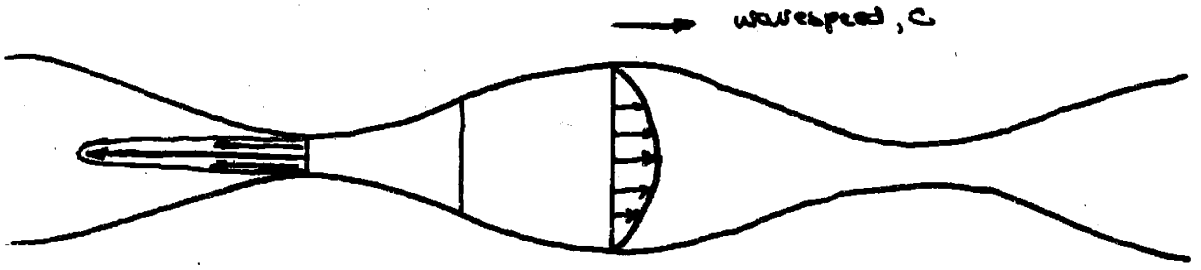

$$T.R. = 0$$

Figure 12

forward over the cycle. Similarly the fluid within the tube will move back and forth, but will make an advance towards the outlet over the course of each cycle. This backward and forward motion occurs even when there is no adverse pressure head across the pump (when T.R. equals $T.R._{max}$). In that case, the back flow at the pinch is just enough so that the associated pressure rise just compensates for the pressure drop of forward flow in the bulge. If an adverse pressure head is placed across the pump, then the back flow will be greater, in order to cause enough additional pressure rise to compensate for the adverse gradient. When the adverse pressure head is so great that no net flow out of the outlet occurs (T.R. equals C), then the fluid within the pump will not make a net advance towards the outlet over the course of a cycle. Of course, the fluid still moves back and forth as the wave passes.

On a qualitative basis (only the sign, not the magnitude or profile), fluid motions within the pump were observed experimentally by introducing dye into the peristaltic tube and watching visually. The observed motions corresponded to the theoretical

expectations outlined above except in one important group of cases. This group was the no net flow situation. The expectation was that no net motion in either direction would occur over the course of a cycle, but that equal amounts of back and forth motion would occur during the cycle. Experimental observations showed that net forward flow occurred in some parts of the tube and net backward in other parts. Specifically, the finite z dimension became a critical factor. At the top and bottom edges of the tube net flow backwards existed. At the middle of the tube net forward flow existed (See figure 12). Cursory efforts to explain this effect did not yield enlightenment.

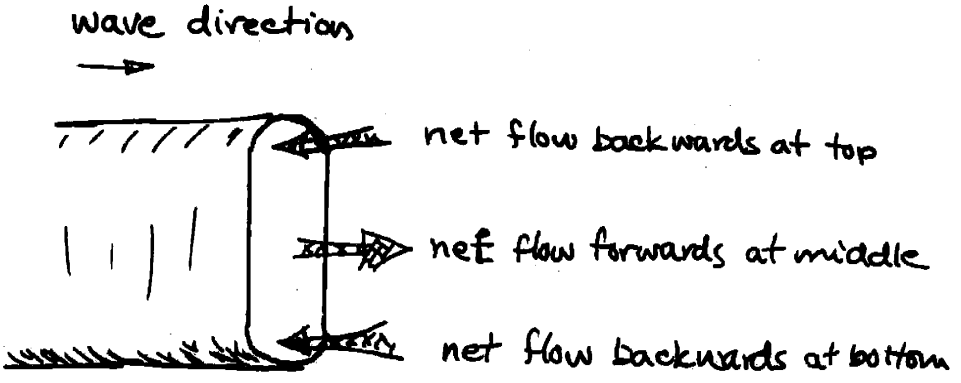

Figure 12

5.4 Secondary Flows

The original purpose of this investigation was to determine if motions causing fluid mixing occur in a peristaltic pump. One way of exploring this area theoretically is to determine the path lines of fluid particles. In a steady system the particle paths are identical to the streamlines, which can be computed if u and v are known. Unfortunately, for a peristaltic pump the laboratory coordinate system is not steady. The position of the streamlines depends upon time. Therefore The path lines must be derived directly by integrating the velocity of the particle with respect to time, getting the particle's position as a function of time. An analytical way of doing this uses the expression for the streamlines in the waveshape (steady) coordinate system, but results in an unmanageable integral (See appendix 4 for details). A second alternative is to integrate the laboratory system velocities over differentially small periods of time using a successive step iteration method. This could be done with either a computer or graphically. In the end none of these alternatives was pursued far enough to yield results.

Efforts were made to measure fluid mixing

experimentally. A salt solution was introduced into the tube at one position and the electroconductivity of the fluid in the tube was measured at another position. However, these experimental efforts were successfully thwarted by capricious fate.

5.5 Conclusion

This investigation has been, at most, an exploratory effort. A reasonable correlation between theory and experiment seems to exist on the gross characteristics of the peristaltic pump. A qualitative correlation exists for the fluid motions within the pump. However, this investigation has not settled the issue of fluid mixing. If one desires to speculate, it seems reasonable that the back and forth motion of the fluid within the pump would cause fluid mixing. If the pump is running at the T.R. equals 0 condition, then one might expect the mixing to be able to transport fluid particles from the pump outlet to the pump inlet in a relatively short time, However, whether this mixing effect is strong enough to buck a net forward flow is not immediately obvious.

6. APPENDIX 1

This appendix will demonstrate the order of magnitude of diffusion in a rat ureter which is not pumping.

From page 391 of Heat, Mass, and Momentum Transfer by Rohsenow and Choi (1961) we get the one dimensional transient diffusion equation:

$$\frac{c}{c_i} = \text{erf}\ \frac{x}{2\sqrt{Dt}}$$

where:

t = time

D = diffusivity

x = distance

c = concentration at x and t

c_i = initial concentration

$c = c_i$ at $t < 0$ for all x

$c = 0$ at $t > 0$ for $x = 0$

Use $D = 3 \times 10^{-5}$ ft^2/hr, a typical figure for diffusion of inorganic materials in water; Take $t = 5$ hours, $x = 1.5$ cm;

Then: $$\frac{c}{c_i} = \text{erf}\ 2.0 = 0.9953$$

Hence the concentration of infection at the kidney after 5 hours will be 0.5% of the concentration at the bladder.

7. APPENDIX 2

7.1 Introduction

This appendix will contain a detailed theoretical analysis of the sinusoidal waveshape and the step waveshape plane two dimensional models. The sinusoidal waveshape case will begin with a derivation of fluid velocities in the waveshape coordinate system. Then it will develop fluid velocities and other quantities in the laboratory coordinate system, including an expression for the pumping characteristics and the Reynolds number. The step waveshape case follows essentially the same lines except that velocity in the y direction is completely neglected. An expression relating analogous dimensionless pumping characteristics is presented for reference.

7.2 Sinusoidal Waveshape Plane Two Dimensional Theory

a) Waveshape Coordinate System:

The waveshape coordinate system is that system which is fixed to the wave and travels with it. The model is shown in figure 13. Note that in this coordinate system the wall moves to the right with constant speed c.

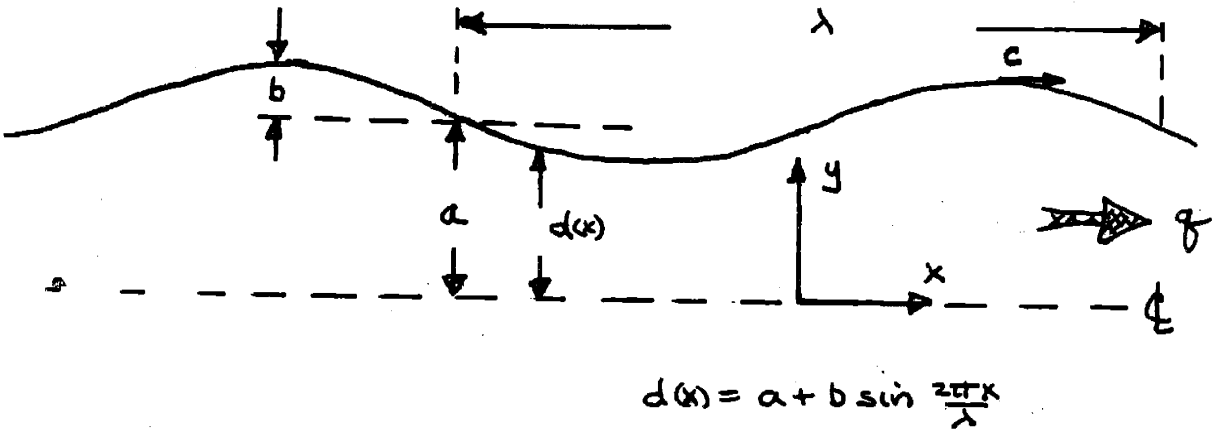

Figure 13

We begin with the most general form of the Navier Stokes equation. If we assume:

1) Gravitational forces are of no consequence;

2) Density is constant over space and time;

3) Viscosity is constant over space and time;

Then the Navier Stokes equation reduces to:

$$\frac{D\underline{V}}{Dt} = -\frac{1}{\rho}\nabla p + \frac{\mu}{\rho}\nabla^2 \underline{V} \qquad \text{Eq. T.1}$$

Where $\underline{V}$ is the vector velocity.

If we take the cartesian form and assume:

4) No z dependence and no z velocity;

5) No time dependence (tube has no ends);

Then we get the forms:

$$u\frac{\partial u}{\partial x} + v\frac{\partial u}{\partial y} = -\frac{1}{\rho}\frac{\partial P}{\partial x} + \frac{\mu}{\rho}\left[\frac{\partial^2 u}{\partial x^2} + \frac{\partial^2 u}{\partial y^2}\right] \qquad \text{Eq 7.2}$$

$$u\frac{\partial v}{\partial x} + v\frac{\partial v}{\partial y} = -\frac{1}{\rho}\frac{\partial P}{\partial y} + \frac{\mu}{\rho}\left[\frac{\partial^2 v}{\partial x^2} + \frac{\partial^2 v}{\partial y^2}\right] \qquad \text{Eq 7.3}$$

Let the symbol $\sim$ represent an order of magnitude relationship. Using order of magnitude considerations, we find:

$$u \sim c \qquad v \sim \frac{b}{\lambda} c$$

$$u\frac{\partial v}{\partial x} \sim \frac{b}{\lambda^2} c^2 \qquad u\frac{\partial u}{\partial x} \sim \frac{c}{\lambda} c$$

$$v\frac{\partial v}{\partial y} \sim \frac{b}{a}\frac{b}{\lambda^2} c^2 \qquad v\frac{\partial u}{\partial y} \sim \frac{b}{a}\frac{c}{\lambda} c$$

$$\frac{\mu}{\rho}\frac{\partial^2 v}{\partial x^2} \sim \frac{\mu}{\rho\lambda}\frac{b}{\lambda^2} c \qquad \frac{\mu}{\rho}\frac{\partial^2 u}{\partial x^2} \sim \frac{\mu}{\rho\lambda}\frac{1}{\lambda} c$$

$$\frac{\mu}{\rho}\frac{\partial^2 v}{\partial y^2} \sim \frac{\mu}{\rho a}\frac{\lambda}{a}\frac{b}{\lambda^2} c \qquad \frac{\mu}{\rho}\frac{\partial^2 u}{\partial y^2} \sim \frac{\mu}{\rho a}\frac{1}{a} c$$

If we assume:

6) Wavelength is long compared to width ($\alpha \ll \lambda$);

7) The width Reynolds number is low ($\frac{\rho u a}{\mu} \ll 1$);

Then:

$$v \ll u$$

$$u \frac{\partial u}{\partial x}, \; v \frac{\partial u}{\partial y}, \; \frac{\mu}{\rho} \frac{\partial^2 u}{\partial x^2} \ll \frac{\mu}{\rho} \frac{\partial^2 u}{\partial y^2}$$

$$u \frac{\partial v}{\partial x}, \; v \frac{\partial v}{\partial y}, \; \frac{\mu}{\rho} \frac{\partial^2 v}{\partial x^2} \ll \frac{\mu}{\rho} \frac{\partial^2 v}{\partial y^2}$$

$$\frac{\mu}{\rho} \frac{\partial^2 v}{\partial y^2} \ll \frac{\mu}{\rho} \frac{\partial^2 u}{\partial y^2}$$

Hence:

$$\frac{\partial p}{\partial x} = \mu \frac{\partial^2 u}{\partial y^2} \qquad \text{Eq 7.4}$$

$$\frac{\partial p}{\partial y} = \mu \frac{\partial^2 v}{\partial x^2}$$

$$\frac{\partial p}{\partial y} \ll \frac{\partial p}{\partial x}$$

Considering these results, we decide to neglect the change of p with respect to y, and to call p a function of x only. Hence, the fluid motions are determined by equation 7.4. The boundary conditions are:

at $y=0$ $\quad \frac{\partial u}{\partial y} = 0$ $\qquad$ at $y=d$ $\quad u=c$ $\qquad$ Eq 7.5

Integration of equation 7.4 with respect to y twice yields :

$$u(xy) = c - \frac{1}{2\mu}\frac{dp}{dx}\left[d^2 - y^2\right] \qquad \text{Eq 7.6a}$$

An alternative form for u, in which dp/dx is replaced by an equivalent expression in terms of q, is more convenient. The relationship between dp/dx and q is found by integrating u with respect to y from 0 to d.

$$q = \int_0^d u\,dy = cd - \frac{1}{3\mu}\frac{dp}{dx}d^3$$

Solving for dp/dx, we get;

$$\frac{dp}{dx} = \frac{3\mu c}{d^2} - \frac{3\mu q}{d^3} \qquad \text{Eq 7.7}$$

The alternative form for u becomes;

$$u = u(xy) = c + \frac{3}{2}\left[\frac{q}{d} - c\right]\left[1 - \frac{y^2}{d^2}\right] \qquad \text{Eq 7.6b}$$

We proceed to find v, using the conditions for continuity and incompressibility, which require;

$$\frac{\partial u}{\partial x} = -\frac{\partial v}{\partial y} \qquad \text{Eq 7.8}$$

The derivative of u (Eq. 7.6b) with respect to x is taken, noting that d is a function of x. Then $\partial u/\partial x$

is integrated with respect to y, using the boundary condition that at $y=0$, $v=0$. The result is:

$$V = \frac{3}{2}\frac{d(a)}{dx}\left[\frac{q}{a}\frac{y}{d} + \left(\frac{2}{3}c - \frac{q}{a}\right)\left(\frac{y^3}{d^3}\right)\right] \quad \text{Eq 7.10}$$

In a steady system the stream function ψ is defined by:

$$\frac{\partial \psi}{\partial x} \equiv v \qquad \frac{\partial \psi}{\partial y} \equiv -u \qquad \text{Eq 7.11}$$

Integration of v with respect to x and u with respect to y leads to the result:

$$\psi = \frac{1}{2}ca\frac{y}{d}\left[\frac{d}{a}\left(1 - \frac{y^2}{d^2}\right) - \frac{q}{ac}\left(3 - \frac{y^2}{d^2}\right)\right] \quad \text{Eq 7.12}$$

b) Laboratory Coordinate System

We shift back to the laboratory coordinate system in order to find the characteristics of the pump. Note that in this coordinate system the wave travels to the left with speed c, and the wall has no y motion. The model for the Laboratory coordinate system is shown in figure 14.

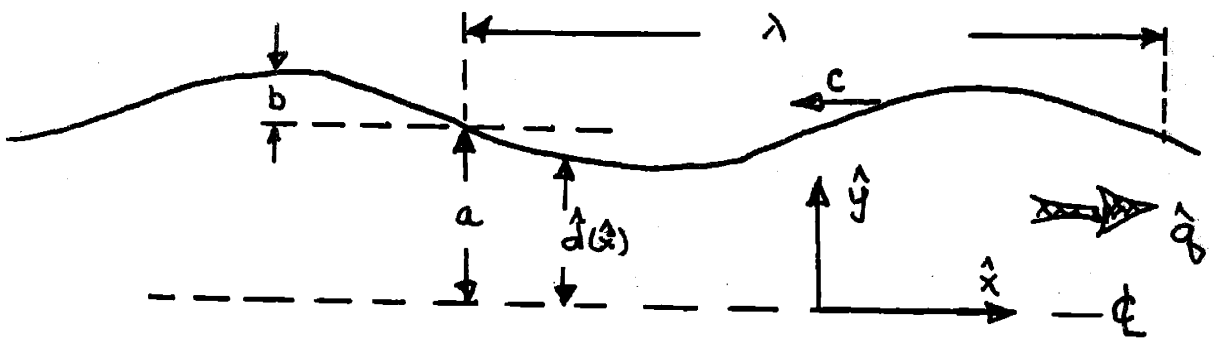

Figure 14

The laboratory coordinate system is related to the waveshape coordinate system by the equations:

$$\hat{x} = x - ct \qquad \hat{y} = y \qquad \text{Eq 7.13}$$

Hence, we have the relations:

$$\hat{d} = d(\hat{x}+ct) = a + b\sin\frac{2\pi}{\lambda}(\hat{x}+ct) \qquad \text{Eq 7.14}$$

$$\hat{q} = q - c\hat{d} \qquad \text{Eq 7.15}$$

$$\hat{u}(\hat{x}\hat{y}) = u(\hat{x}+ct, \hat{y}) - c = \frac{3}{2}\left[\frac{q}{d} - c\right]\left[1 - \frac{\hat{y}^2}{\hat{d}^2}\right] \qquad \text{Eq 7.16a}$$

$$\hat{v}(\hat{x}\hat{y}) = v(\hat{x}+ct, \hat{y}) = \frac{3}{2}\frac{d(\hat{d})}{d\hat{x}}\left[\frac{q}{d}\frac{\hat{y}}{\hat{d}} + \left(\frac{2}{3}c - \frac{q}{d}\right)\left(\frac{\hat{y}^3}{\hat{d}^3}\right)\right] \qquad \text{Eq 7.16b}$$

$$\hat{\psi}(\hat{x}\hat{y}) = \frac{1}{2}ca\frac{\hat{y}}{\hat{d}}\left[\frac{\hat{d}}{a}\left(1 - \frac{\hat{y}^2}{\hat{d}^2}\right) - \frac{q}{ac}\left(3 - \frac{\hat{y}^2}{\hat{d}^2}\right)\right] \qquad \text{Eq 7.17}$$

An interest in the gross characteristics of the pump compels us to develop a relationship between the dimensionless pressure rise and the dimensionless output flow. First, we call the dimensionless flow the transport ratio, and define it as the ratio of the net volume output during a cycle to an arbitrarily selected reference volume. We choose the reference volume to be the volume contained under the bulge, represented by the shaded area in figure 15.

Figure 15

Hence, we represent the transport ratio as:

$$T.R. = -\frac{\int_{t_0}^{t_0+\frac{\lambda}{c}} \hat{q}\, dt}{b\lambda} = \frac{aL - q\frac{\lambda}{c}}{b\lambda} = \frac{a}{b}\left[1 - \frac{q}{ac}\right] \quad \text{Eq 7.18}$$

The minus sign in front of the first expression is so that we measure flow towards the left, in the direction of the wave motion. From this relationship we notice that the transport ratio is zero (no net flow) when $q = ac$.

The pressure rise across a wavelength will be

the same in both coordinate systems. Integration of equation 7.7 with respect to x over one wavelength gives the expression:

$$\Delta P_x^{x+\lambda} = 3\mu c \int_x^{x+\lambda} \frac{dx}{\left(a+b\sin\frac{2\pi x}{\lambda}\right)^2} - 3\mu q \int_x^{x+\lambda} \frac{dx}{\left(a+b\sin\frac{2\pi x}{\lambda}\right)^3} \qquad \text{Eq 7.19}$$

Evaluation of the integrals on the right leads to:

$$\Delta P_x^{x+\lambda} = \frac{3\mu\lambda}{a^3} \frac{1}{\left(1-\frac{b^2}{a^2}\right)^{5/2}} \left[ca\left(1-\frac{b^2}{a^2}\right) - q\left(1+\frac{b^2}{2a^2}\right)\right] \qquad \text{Eq 7.20}$$

We define a pressure ratio as the ratio between the pressure rise across one wavelength to an arbitrarily selected reference pressure rise. We choose the reference pressure rise to be the pressure rise that occurs across one wavelength when there is no net flow (T.R. = 0). For this condition, as noted above, q = ac, and equation 7.20 gives:

$$\Delta P_{x\,max}^{x+\lambda} = \frac{3\mu\lambda}{a^3} \frac{1}{\left(1-\frac{b^2}{a^2}\right)^{5/2}} \left[-\frac{3}{2}\frac{cb^2}{a}\right] \qquad \text{Eq 7.21}$$

This pressure rise is the largest one that the pump can produce. The pressure ratio becomes:

$$P.R. \equiv \frac{\Delta P_x^{x+\lambda}}{\Delta P_{x\,max}^{x+\lambda}} = -\frac{2}{3}\frac{a^2}{b^2}\left[\left(1-\frac{b^2}{a^2}\right) - \frac{q}{ac}\left(1+\frac{b^2}{2a^2}\right)\right] \qquad \text{Eq 7.22}$$

Combination of equation 7.18 and 7.22, and elimination of q yields a relationship between T.R., P.R., and geometric factors.

$$T.R. = \frac{a}{b}\left[\frac{3}{2\frac{a^2}{b^2}+1}\right]\left[1 - P.R.\right] \qquad \text{Eq } 7.23$$

For normal pumping, P.R. falls in the range $0 \leq P.R. \leq 1$ and T.R. has the corresponding range $\frac{a}{b}\left[\frac{3}{2\frac{a^2}{b^2}+1}\right] \geq T.R. \geq 0$. Equation 7.23 shows the linear relationship between T.R. and P.R. In particular, it says that the transport ratio is merely a constant term which is the maximum transport ratio minus a seepage term which is directly proportional to the adverse pressure head.

c) Reynolds Number

In its differential form, Reynolds number is:

$$\text{Reynolds number} = \frac{\text{inertial forces}}{\text{viscous forces}} = \frac{\rho u \frac{\partial u}{\partial x}}{\mu \frac{\partial^2 u}{\partial y^2}} \qquad \text{Eq } 7.24$$

If we evaluate this expression formally, using u in equation 7.6b, we find that the Reynolds number ranges from 0 to infinity depending upon what position along the tube is selected. The physical reason for this result is that the inertial forces vanish as some positions and the viscous forces at others. Hence, we attempt to establish a meaningful guidepost by

computing the maximum inertial forces and maximum viscous forces along the tube separately. The order-of-magnitude Reynolds number will then be their ratio.. From equation 7.6b, we have:

$$u = c + \frac{3}{2}\left[\frac{q}{d} - c\right]\left[1 - \frac{y^2}{d^2}\right]$$

Where q is related to T.R. by:

$$q = c\left[a - b\,T.R.\right]$$

Physical reasoning tells us that the maximum inertial effects will occur along the centerline of the tube. Evaluating the terms in the numerator along the centerline, we get:

$$u_{\ell} = \frac{3}{2}c\left[\frac{a}{d} - \frac{b}{d}T.R. - \frac{1}{3}\right]$$

$$\frac{\partial u}{\partial x}_{\ell} = -\frac{3}{2}c\left[\frac{a}{d} - \frac{b}{d}T.R.\right]\frac{d(d)}{dx}$$

Evaluating the terms in the denominator we have:

$$\frac{\partial^2 u}{\partial y^2} = -\frac{3c}{d^2}\left[\frac{a}{d} - \frac{b}{d}T.R. - 1\right]$$

Physical reasoning shows that for normal pump operation the inertial forces are greatest at the position d = a, whereas the viscous forces are greatest at position d = a-b. Evaluating the numerator and denominator at these positions and using $d(d)/dx = -4b/\lambda$ at d = a, we get a final expression:

$$\text{Reynolds } \# = \frac{\rho c (a-b)}{\mu} \frac{a-b}{a} \frac{a-b}{\lambda} \frac{3\left[\frac{2}{3} - \frac{b}{a} T.R.\right]\left[1 - \frac{b}{a} T.R.\right]}{\left[1 - T.R.\right]} \quad \text{Eq 7.25}$$

7.3 Step Waveshape Plane Two Dimensional Model

This model will not be presented with as much detail as the sinusoidal waveshape model since it did not receive as much attention during the investigation. The main purpose of this section will be to write down the results for reference.

Again we start with the waveshape coordinate system, which is fixed to the wave and travels with it. In this system the wall is moving towards the right with speed c. The model is shown in figure 16.

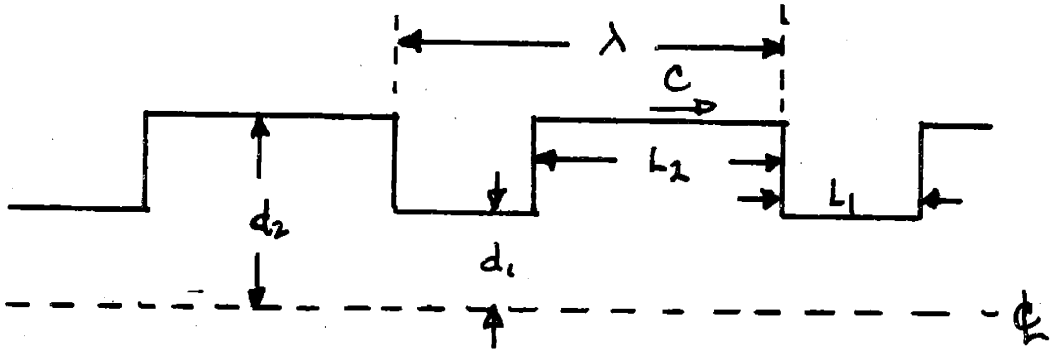

Figure 16

We make the same assumptions we did in the previous case.

1) Gravitational forces are of no consequence;
2) Density is constant over time and space;
3) Viscosity is constant over time and space;
4) No z dependence and no z velocity
5) No time dependence;

Again the Navier Stokes equation is reduced to the forms of equation 7.2 and 7.3. However, because of the discontinuity associated with the step waveshape, we will not try to handle the detailed motion of the fluid within the pump for this model. Specifically, we neglect velocities in the y direction altogether. We are left with equation 7.2:

$$u\frac{\partial u}{\partial x} + v\frac{\partial u}{\partial y} = -\frac{1}{\rho}\frac{\partial P}{\partial x} + \frac{\mu}{\rho}\left[\frac{\partial^2 u}{\partial x^2} + \frac{\partial^2 u}{\partial y^2}\right] \quad \text{Eq. 7.2}$$

We desire to test the order of magnitude of the viscous term and the inertial term. If we carry out an order of magnitude integration of this expression with respect to x across one wavelength, we get for the pressure rise across the wavelength:

$$\Delta P_x^{x+\lambda} \sim \frac{\mu c \Delta}{d^2} - \rho c^2$$

If we assume:

6) Width Reynolds number is low ($\frac{3\omega d}{\mu} \ll 1$)

7) Wavelength is long compared to width ($d \ll \lambda$)

Then:

$$\frac{\rho c^2}{\frac{\mu c l}{d^2}} = \frac{\rho c d}{\mu} \frac{d}{\lambda} \ll 1$$

Hence we may neglect the inertial term, and use the form:

$$\frac{\partial P}{\partial x} = \mu \frac{\partial^2 u}{\partial y^2}$$

Thus, the implication of these assumptions is that all departures from parabolic Poiseuille flow are insignificant. After a derivation analogous to the preceding one, we find a relationship between the transport ratio and the pressure ratio:

$$T.R. = \frac{\left[1 - \frac{d_1}{d_2}\right]^2 \left[\frac{d_1^3}{d_2^3} - 1\right]}{\frac{L_2}{\lambda - L_2} \frac{d_1^3}{d_2^3} + 1} \left[1 - P.R.\right] \qquad \text{Eq 7.26}$$

Where the definition of the transport ratio is the volume transported in one cycle divided by the volume under the bulge, shown by the shaded area in figure 17;

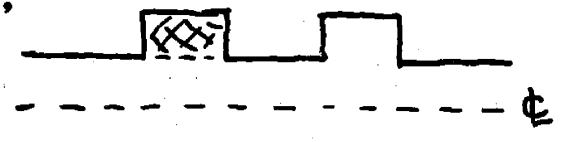

Figure 17

And where the pressure ratio is defined as the pressure rise across one wavelength divided by the pressure rise across one wavelength when T.R. equals 0. This is the maximum pressure rise the pump can produce, and is given by:

$$\Delta P_{x}^{x+\lambda}{}_{max} = 12\mu L_2 \left[\frac{L_2}{d_1}\right]^2 \frac{d_2}{d_1} \frac{\lambda - L_2}{L_2} \left[\frac{d_1}{d_2} - 1\right]\left[\frac{d_1^3}{d_2^3} - 1\right] \quad \text{Eq 7.27}$$

8. APPENDIX 3, EXPERIMENTAL APPARATUS

This appendix will give some detailed information about the experimental apparatus. It will discuss the various components, giving dimensions, and outlining the operating range.

a) The Tube and Wave Forming Components

A top view of the tube and the wave forming components are shown in figure 18.

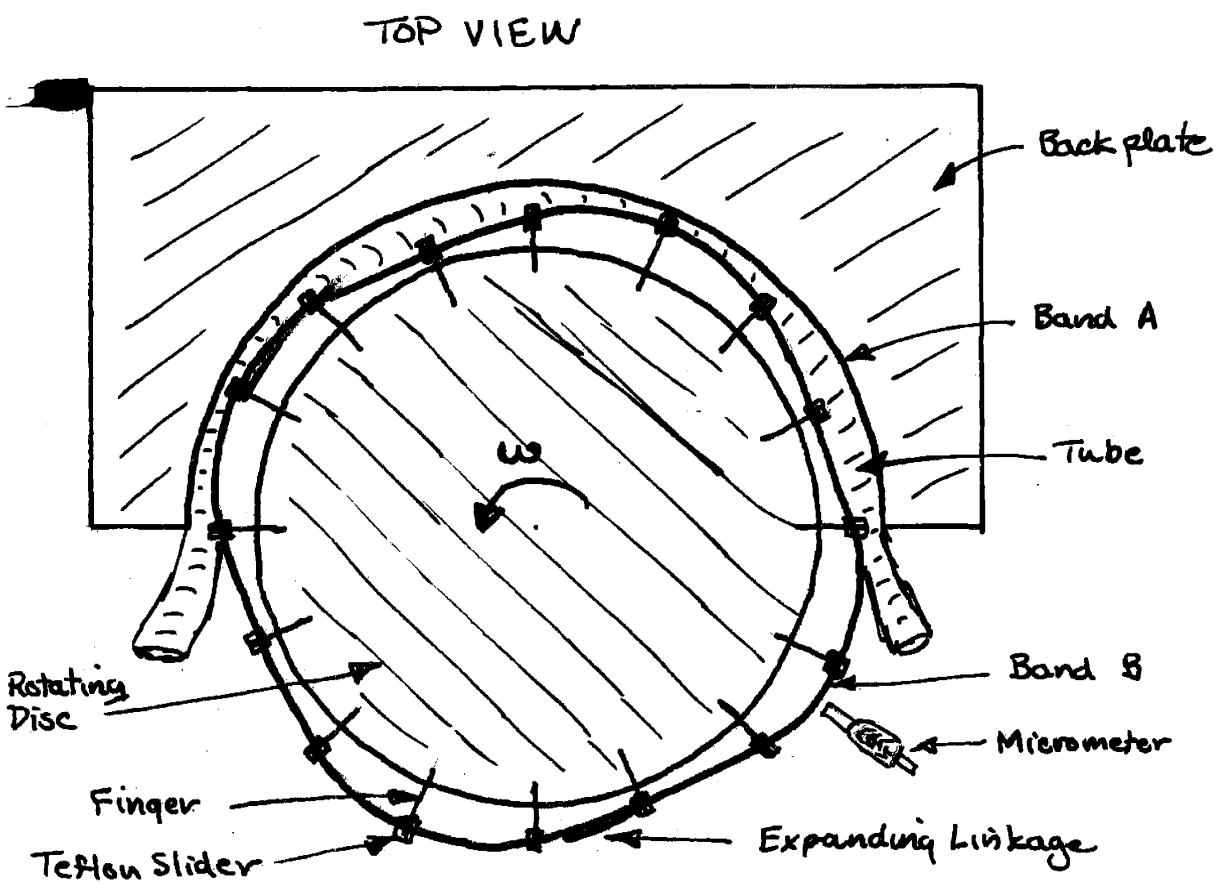

Figure 18

The tube was clear polyvinylchloride. Its dimensions were; wall thickness, 0.050"; average width, 0.3"; length, 45"; depth, 2.5". The tube was constrained between two spring steel bands. The bands were 3" wide and 0.015" thick. Band A was fixed to a rigid piece of flakeboard,and formed a semi-circle. The radius of the semi-circle was about 16". The out-of-round tolerance was about 0.010". The tube was cemented to band A. Band B constrained the other side of the tube, and was responsible for the squeezing wave motion. It was supported by the teflon sliders on fingers which were mounted on the rotating disc. For a larger scale diagram of the fingers, see figure 19.

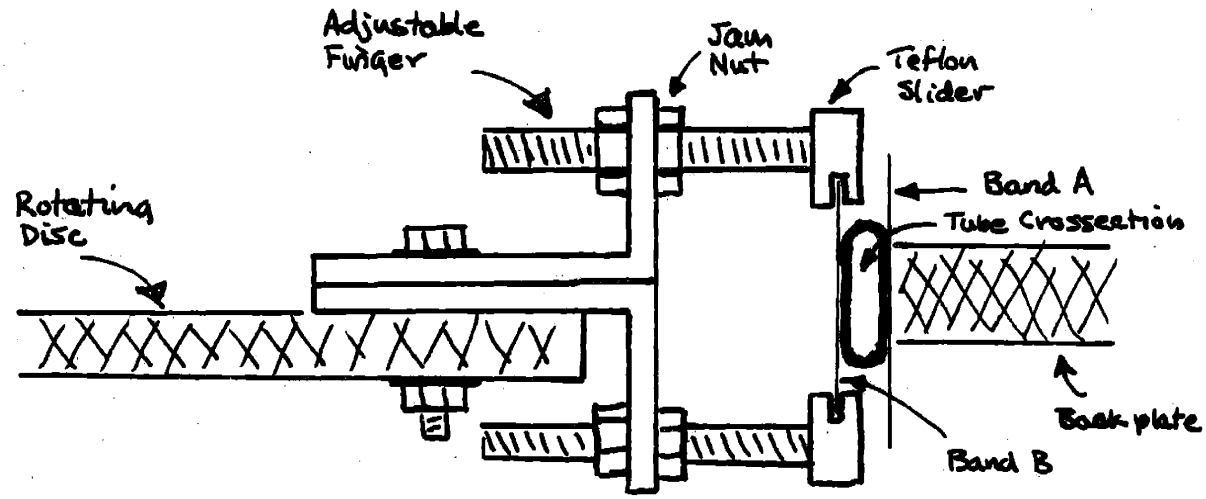

Figure 19

The 64 adjustable fingers could be set for a variety of wave geometries. Two micrometers were used to measure the adjustment. The tolerance of adjustment was about 0.020". Neither band A nor band B could rotate. As the disc rotated, the fingers slid along band B, thus causing the waveshape determined by the fingers to move along the tube. An expanding linkage in band B allowed the sliders to pass easily, yet allowed changes in the total perimeter of band B. The disc could rotate from 0.2 rpm to 10 rpm. The corresponding wavespeeds were 1 cm. per second to 50 cm. per second. The disc was driven by a $\frac{1}{4}$ horsepower D.C. motor. Speed variation was produced by varying the voltage across the armature. Figure 20 is a schematic representation of how the tube was connected to the reservoirs.

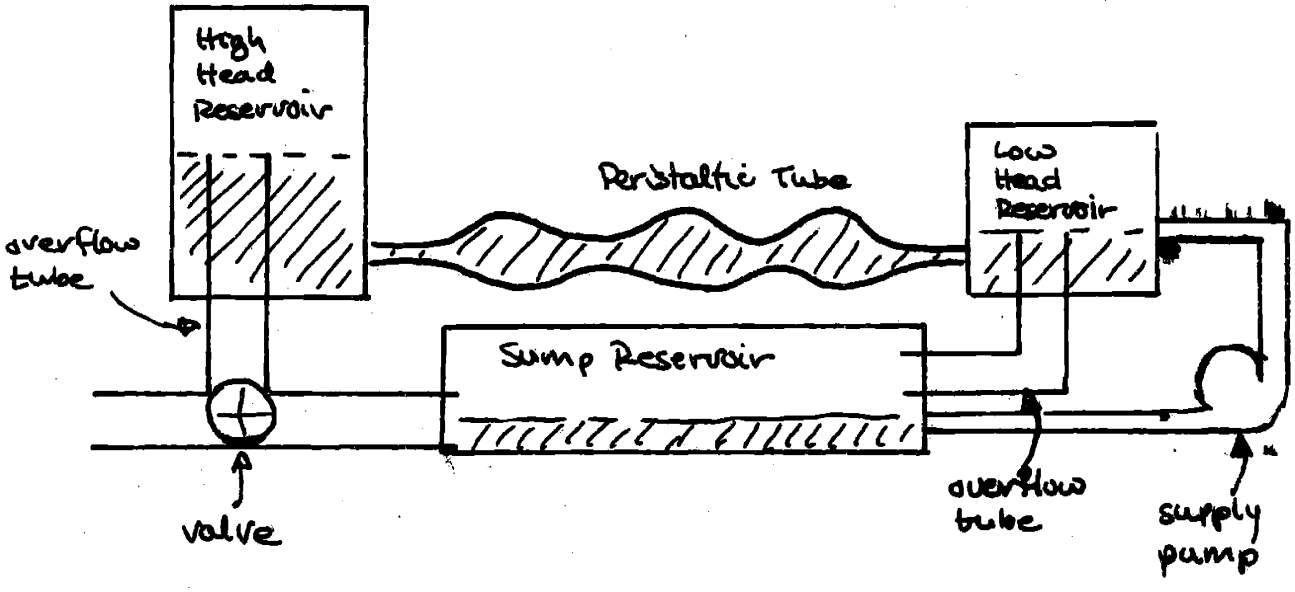

Figure 20

Both reservoirs were 6" in diameter, so that periodic flow fluctuations inherent to the peristaltic pump would not cause significant pressure head fluctuation. The fluid level in the low head reservoir was held constant by means of a supply pump and overflow tube arrangement. The flow rate of the supply pump was enough so that the fluid was continuously spilling over into the overflow tube. The pressure rise across the peristaltic pump was determined by the height of the overflow tube in the high head reservoir, which could be varied. This height was measured. The fluid which overflowed into this tube represented the net flow of the peristaltic pump and was measured volumetrically. For this purpose a valve was placed on the high head reservoir overflow tube, which controlled whether the overflow went to a graduated cylinder or to the sump reservoir. The overflow tubes were 1" in diameter. The maximum pressure head allowable was about 12 inches of fluid. The working fluids of the experiment were corn syrup in some cases, glycerine in others. On the whole, the glycerine was more satisfactory. The viscosity ranged from 250 centipoises to 3 centipoises. The viscosity was measured with a standard viscometer. Photographs 1 and 2 show the apparatus from different angles. Photograph 1 was taken from behind and above the apparatus. Photograph 2 was taken from in front of the apparatus.

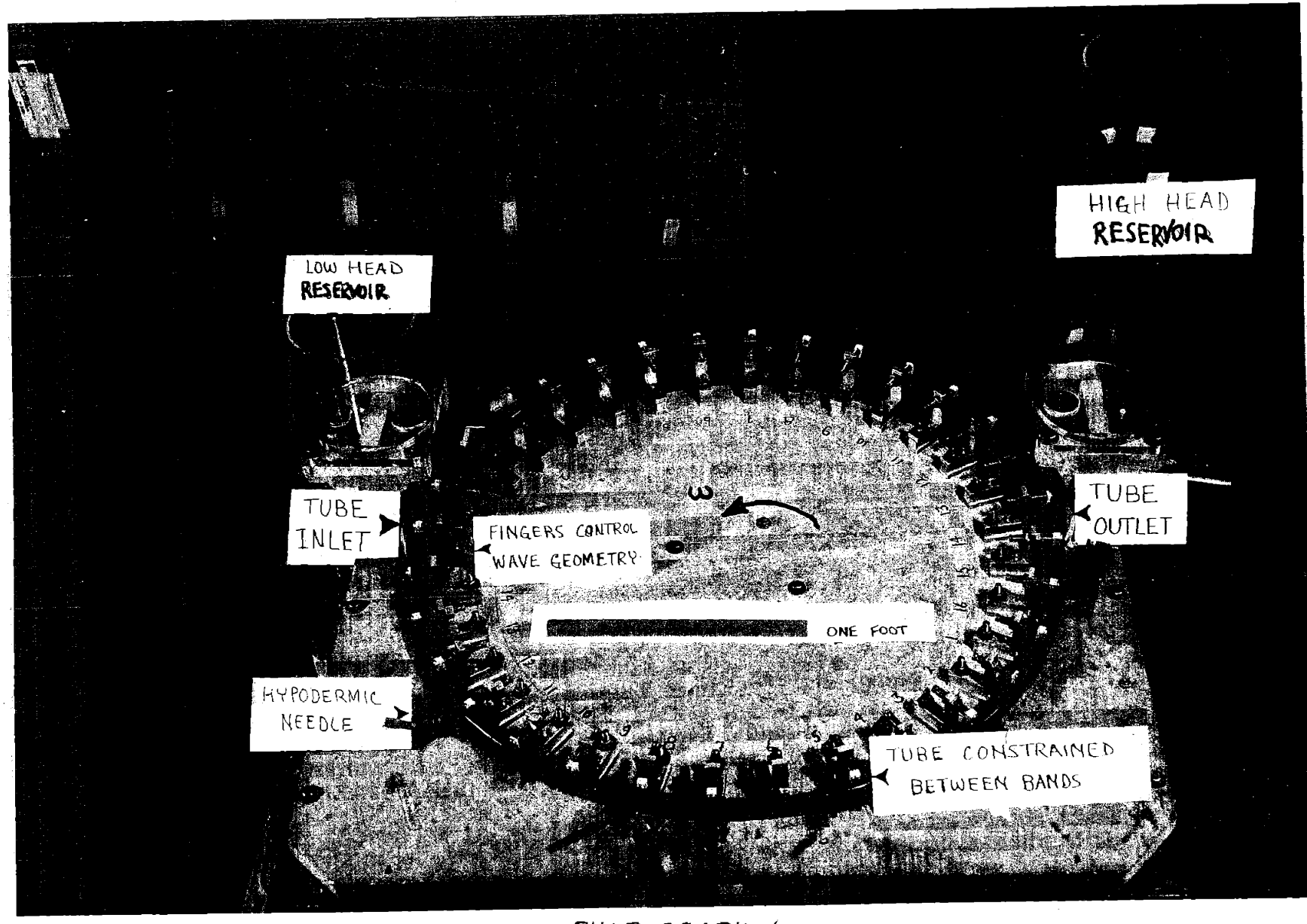

PHOTOGRAPH 1

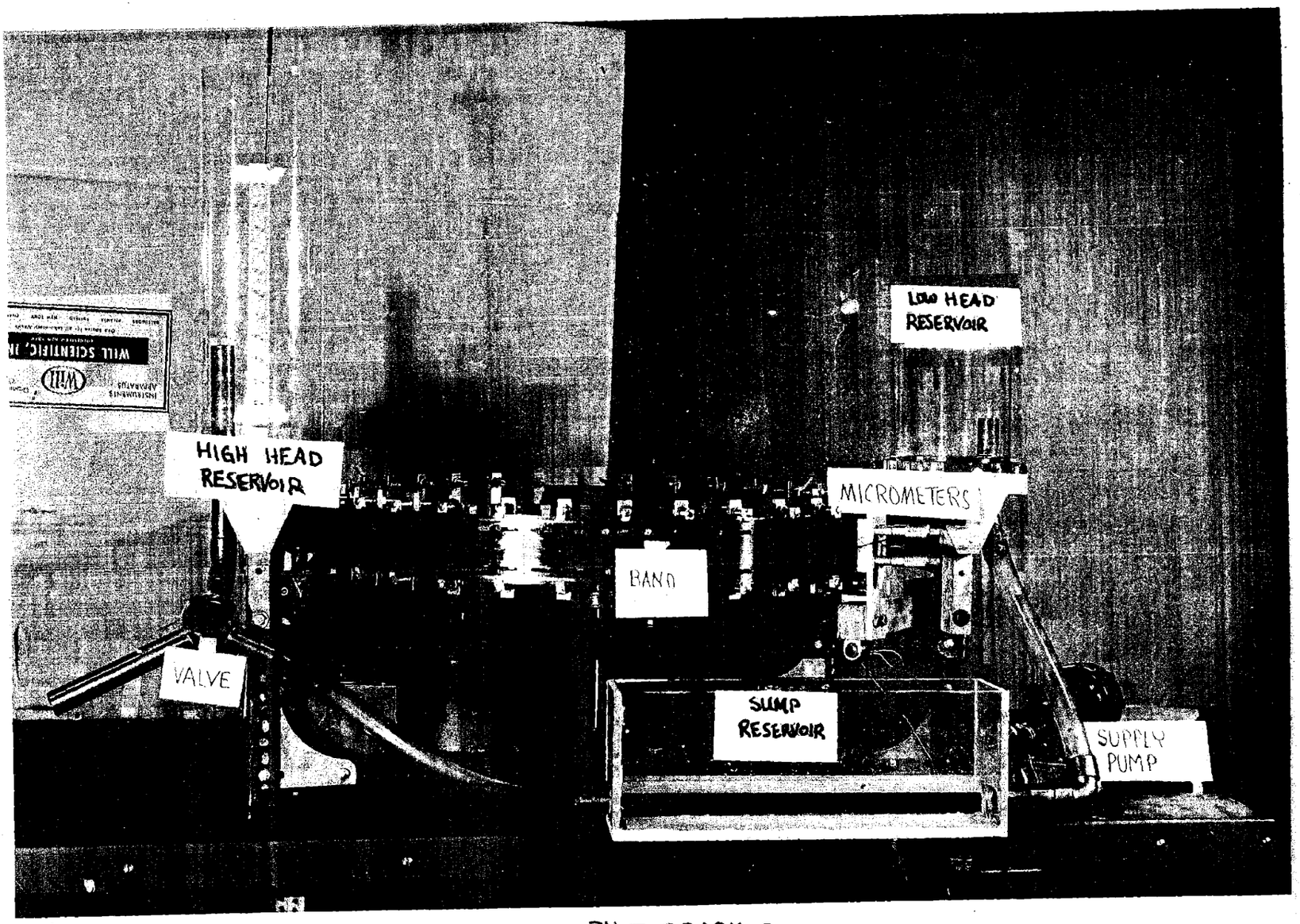

PHOTOGRAPH 2

9. APPENDIX 4, PATH LINES

This appendix will describe an analytic way of finding particle path lines for the sinusoidal plane two dimensional model.

Let us establish the following nomenclature:

space coordinates waveshape system	x y	space coordinates laboratory system	$\hat{x}$ $\hat{y}$
particle coordinates waveshape system	ξ η	particle coordinates laboratory system	$\hat{\xi}$ $\hat{\eta}$

We desire to find the particle position as a function of time, i.e. $\hat{\xi} = \hat{\xi}(t)$ and $\hat{\eta} = \hat{\eta}(t)$, since the path lines are described by the successive particle positions over time. We observe that if $\xi(t)$ and $\eta(t)$ are known, then $\hat{\xi}(t)$ and $\hat{\eta}(t)$ follow directly from the relations:

$$\hat{\xi}(t) = \xi(t) - ct \qquad \hat{\eta}(t) = \eta(t) \qquad \text{Eq 9.1}$$

We set ourselves the task of finding $\xi(t)$ and $\eta(t)$. At every point in space the velocities of the particle will coincide with the space coordinate velocity at that position. Hence:

$$\frac{\partial \xi}{\partial t} = u(\xi, \eta) \qquad \frac{\partial \eta}{\partial t} = v(\xi, \eta) \qquad 9.2$$

Where u and v are the velocities defined in space coordinates by equations 7.6b and 7.10. Solving equation 9.2 directly would involve solving two simultaneous integral equations. We can avoid this unfavorable situation by using the fact that in the waveshape coordinate system, which is steady, the stream lines and path lines are identical. The particle will be on a particular stream line, which is identified by the associated constant value of the stream function, ψ_p. For that stream line, a relationship exists between η and ζ in terms of ψ_p, given by equation 7.12. Manipulation leads to isolation of η, giving η in terms of ζ and ψ_p.

$$\eta = \eta(\zeta, \psi_p) \qquad \text{Eq } 9.3$$

We use this to reduce $u(\zeta,\eta)$ to a function of ζ and ψ_p only. Then equation 9.2 becomes:

$$\frac{\partial \zeta}{\partial t} = u\left[\zeta, \eta(\zeta \psi_p)\right] = u(\zeta, \psi_p \text{ only}) \qquad \text{Eq } 9.4$$

Since the term on the right contains only ζ and constants, we have reduced the simultaneous integral equations to a single integral equation. We can separate the variables and integrate to find a relationship between ζ and t.

$$\int_{\zeta_0}^{\zeta} \frac{\partial \zeta}{u(\zeta)} = \int_{T_0}^{T} dt \qquad \text{Eq } 9.5$$

The relationship will involve ψ_p, which states which stream line the particle travels on; and ξ_0 and T_0, which state the x position of the particle at time T_0. Collectively, these three constants define the identity of the particle.

If we carry out these operations with the actual functions, we find that the left integral in equation 9.5 is impossible to handle analytically. Equation 7.12 gives us:

$$\psi_p = \tfrac{1}{2} ca \frac{\eta}{d}\left[\frac{d}{a}\left(1-\frac{\eta^2}{d^2}\right) - \frac{g}{ac}\left(3-\frac{\eta^2}{d^2}\right)\right] \qquad \text{Eq 9.6}$$

where;

$$d = a + b\sin\frac{2\pi\xi}{\lambda}$$

Hence:

$$\eta^3 + \frac{(c - 3g/d)}{(g/d^3 - c/d^2)}\eta - \frac{\psi_p}{g/d^3 - c/d^2} = 0$$

Finding η as a function of ψ_p and ξ, we have:

$$\eta = \left[\frac{\psi_p}{s} + \sqrt{\frac{\psi_p^2}{s} + \frac{(c-3g/d)^3}{27s^3}}\right]^{1/3} - \frac{c - 3g/d}{3s\left[\frac{\psi_p}{s} + \sqrt{\frac{\psi_p^2}{s} + \frac{(c-3g/d)^3}{27s^3}}\right]^{1/3}} \qquad \text{Eq 9.7}$$

where;

$$s = \frac{g}{d^3} - \frac{c}{d^2}$$

From equation 7.6b we have:

$$u = u(\xi,\eta) = c + \frac{3}{2}\left[\frac{g}{d} - c\right]\left[1 - \frac{\eta^2}{d^2}\right] \qquad \text{Eq 9.8}$$

Substitution of 9.7 into 9.8 would give u as a function of ζ only. It is clear from this demonstration, however, that $\int_{\zeta_0}^{\zeta} \frac{d\zeta}{u(\zeta)}$ could not be handled by analytic methods.

FOOTNOTES

1) Webster's New Collegiate Dictionary, pg 627; G & C Merriam Co., 1959:

2) Dr. Kass, personal communication:

3) Most of this information was taken from: The Function of the Ureter and Renal Pelvis, Fredrik Kiil; Oslo University Press, W.B. Saunders Co., 1957:

4) "Surgical Physiology of the Renal Pelvis and Ureter", Saul Boyarsky; Monographs in the Surgical Sciences, June, 1964, pg 181:

BIBLIOGRAPHY

The following references are useful mainly to the extent that they give the layman a rough idea of how the ureter acts.

1) The Function of the Ureter and Renal Pelvis, Fredrik Kiil; Oslo University Press, W. B. Saunders Co., 1957: I found this book by far the most useful because it had a series of radiographic pictures of the ureter and because a lot of data about the normal operating characteristics of the ureter were given.

2) "The Response of the Ureter and Pelvis to Changing Urine Flows", Pablo A. Morales et alia; The Journal of Urology, Vol 67, No. 4, April, 1952: Observation of the ureter of an unanesthetized dog under varying urine flows.

3) "Zur Physiologie des Ureter", Engelmann; Archiv Fur die Gesmte Physiologie, Vol II, pg 243-293: Englemann was one of the first to make a thorough study of the ureter.

4) "Surgical Physiology of the Renal Pelvis and Ureter", Saul Boyarsky; Monographs in the Surgical Sciences, June, 1964: A valuable article because, if for no other reason, it has a listing of about 200 references in the bibliography.